Active and Passive Mixing for Immiscible Liquid-Liquid Systems: A Performance Evaluation of Novel Micro-Reactors

By Sébastien Mongeon

Thesis submitted to the Faculty of Graduate and Postdoctoral Studies
in partial fulfillment of the requirements for the degree of

Master of Applied Science (MASc)

in Chemical Engineering

Department of Chemical and Biological Engineering
Faculty of Engineering

uOttawa

University of Ottawa

Abstract

Continuous flow reaction using micro-reactors is a valued technology due to its excellent mass and heat transfer performance, reduced reactor volume, handling capacity of hazardous reactions, and many other process intensifications. These intensifications opportunities interest the fine chemicals, pharmaceuticals producers and other multiphase reaction users who currently use batch processes or already use continuous flow. In this thesis, elements of passive and active mixing are investigated for the application of immiscible liquid-liquid systems.

In the first study, the effects of geometrical arrangements of a residence time between mixing units on the interphase mass transfer rates are evaluated with four different immiscible liquid-liquid systems. A presentation of an algorithm for the optimal selection of a reactor and its operating conditions is given in order to enable easy and improved use of one's micro-reactor.

In the second study, the impact of a secondary pulse flow on interphase mass transfer is investigated. A coil without internal baffles is used as the oscillatory-flow coil reactor with a continuous active mixing source. The best application for the reactor is determined using a comparison to other complementary continuous flow platforms in the toolbox approach.

The novel advancements presented here will help lead new molecular discoveries and connect the laboratory science scale to the process engineering production scale.

Résumé

La production en continue via micro-réacteurs est appréciée pour ses nombreuses opportunités d'intensifications de procédés : qualités en transfert de masse et thermique, réduction du volume de réacteur, capacités à traiter des réactions avec matières dangereuses, etc. Ces opportunités sont d'intérêt aux industries pharmaceutiques, chimiques et utilisateurs des réactions polyphasées. Des éléments de mélange passif et actif sont étudiés dans cette thèse pour l'application des systèmes liquide-liquide immiscibles.

La première étude présente l'analyse d'un micro-réacteur à plaque utilisant des éléments de mélange statiques. Les effets des dispositions géométriques d'un canal de temps de séjour sur les taux de transfert de masse entre phases sont évalués pour quatre paires de systèmes liquide-liquide immiscibles. Un algorithme de sélection pour l'application optimal d'un réacteur de ce type est introduit afin de faciliter et améliorer son utilisation dans plusieurs circonstances.

La deuxième étude détaille l'impact d'un mélange actif à impulsions secondaires sur le transfert de masse entre phases. Un tube sans chicanes est utilisé comme réacteur à serpentin avec une pompe doseuse comme source de mélange actif. La meilleure application pour le réacteur est déterminée à l'aide d'une comparaison avec d'autres plates-formes complémentaires de production en continu.

Les progrès novateurs présentés aideront à avancer de nouvelles découvertes moléculaires ainsi qu'à joindre la science du laboratoire à l'ingénierie des procédés.

Declaration of Contributors

I hereby declare that I am the sole author of this thesis. My supervisor, Dr. Arturo Macchi and co-supervisor, Dr. Dominique Roberge, provided comments and editorial corrections throughout my work. This work would not have been possible without them.

The experimental plan of Sections 2 was designed by me while at the R&D laboratories of Lonza AG. The initial design of the micro-mixing unit LL-Rhombus used was initiated by Dr. Patrick Plouffe. I designed the geometrical arrangements of the micro-reactor plates and prepared the CAD. The micro-reactor plates were manufactured by Ehrfeld Mikrotechnik BTS. The experiments were performed at Lonza AG in Visp, Switzerland by Eric Mielke and I with the technical help of Sarah Filliger, and Michael Bittel, employees at Lonza. The article is co-authored with Eric Mielke and guidance was given by Dr.Patrick Plouffe, both of which are listed as co-authors.

The experimental plan of Sections 3 was designed by me while at the R&D laboratories of Lonza AG. The reactor system was designed with the assistance of Dr. Petteri Elsner, Michael Bittel, Dr. Dominique Roberge. I performed the experiments at Lonza AG in Visp, Switzerland with the technical help of Anton Pfammatter and Michael Bittel, Lonza employees.

Acknowledgements

Professional

I express gratitude for the possibilities that have been given to me by both my thesis supervisor and co-supervisor, Dr. Arturo Macchi and Dr. Dominique Roberge. The knowledge, experiences, help and guidance that you have given me have greatly provided to my success. I thank Dr. Patrick Plouffe for sharing his brilliance and time with me; I always enjoy our conversations. Eric Mielke, I recognise your great support, help and critical thinking that you brought to the research.

I would like to thank Lonza AG for the partnership between the private sector and the higher education institutions. I acknowledge the financial support of Lonza AG, the NSERC Continuous Flow CREATE program, and the University of Ottawa.

Personal - Friendship

I would like to note the wonderful friendships made at the University of Ottawa during this time: Nicolas Brazeau, Benoit Duhoux, Francis Kus, Maxime Lortie, Eric Mielke, Jordan O'Reilley, Valois Parisien, Patrick Plouffe and Ryad Rahman. I always enjoy our conversations. I raise my glass to the adventures and delights lived in Switzerland with new friends and colleagues: Kay Ake-Locke, Marvin Bachmann, Jared Bodecker, Firat Canbay, Markus Füreder, Clément Goua de Baix, Hiromu Hattori, Nils Holgersson, Manuel Stark, Anatol Tumencev, Mareike Perzborn, Michaela Reichinger, Simon Reifenschweiler, Gilles Richner, Carole Schöpfer, Jan Skula.

Personal - Family

Thank you to my parents, Jean and Carole Mongeon, and my family. The time, love, and patience that you have so generously devoted to me helped make each step possible.

I lastly give the biggest of thank you to my partner, Myriam Couture. You are insightful, determined, and inspiring; you help me succeed and discover new realities in and out of my studies. Your encouragements have and continue to make a positive impact on me. I profoundly appreciate and love you.

Remerciements personnels - Famille

Merci à mes parents, Jean et Carole Mongeon, ainsi qu'à ma famille. Le temps, l'amour et la patience que vous m'avez si généreusement accordés ont contribué à rendre chaque étape possible.

Je donne le plus grand des remerciements à mon amour, Myriam Couture. Tu es perspicace, déterminée et inspirante; tu m'aides à réussir et découvrir de nouvelles expériences dans mes études, mon travail et ma vie personnelle. Tes encouragements ont eu et continuent d'avoir un impact positif sur moi. Je t'aime et t'apprécie énormément.

Table of Contents

List of Figures

List of Tables

1 Introduction

1.1 Background

Multiple reactions using partially or totally immiscible[1] liquid-liquid systems such as alkali-catalysed transesterification [1–3], benzylation [4], and nitration [5] are of interest to the fine chemical and pharmaceutical industry. A pharmaceutical producer requires the ability to produce at the smaller scale of milligrams/grams/kilograms through the pre-clinical and Phase I, and quickly increase the production to the several kilograms up to tons for Phase II and III. The increase is needed to cover the growing number of people required in the test phases. The US Federal Drug Administration requires that 20 to 100 people be evaluated in Phase I, several hundred in Phase II, and 300 to 3,000 in Phase III.[6] It is of importance that in the product process development speed, quality, risk assessment, and costs are considered.[7] Phase II failure rate is almost double that of Phase I and Phase III in drug development with 68% versus 35% and 40% respectively.[8] A promising drug can be stopped from reaching phase III because an over or under-engineered and non-scalable process is used, whereas an efficient process development and optimisation with low costs can rapidly advance the drug approval.

An issue encountered during the product development using an immiscible liquid-liquid reaction is the limited contact area between phases. Mass transfer limitations are apparent when the laboratory batch or semi-batch process scale-up approach is used.

[1] Partially or totally immiscible will be abridged with immiscible for the sake of brevity.

The mixing mechanism utilised at the pre-clinical milligrams/grams production stages are no longer viable. The solution of a lengthier campaign is undesirable in order to continue on to the kilograms production. A change in design concept is then required which increases the steps and time in the product scale-up process development.

Continuous flow reaction using micro-reactors at the laboratory scale solves the scale-up issue by reducing the re-design needed to bring the reaction to the production scale. A constant input and output feed with no internal accumulation is used in order to achieve a steady state. Critical process parameters can then be readily identified by changing steady state. The approach allows a design of experiment to be completed in less time than using a batch approach. Appropriate control strategies are established for these critical process parameters. An example of a typical continuous flow reaction setup is shown in Figure 1.1.

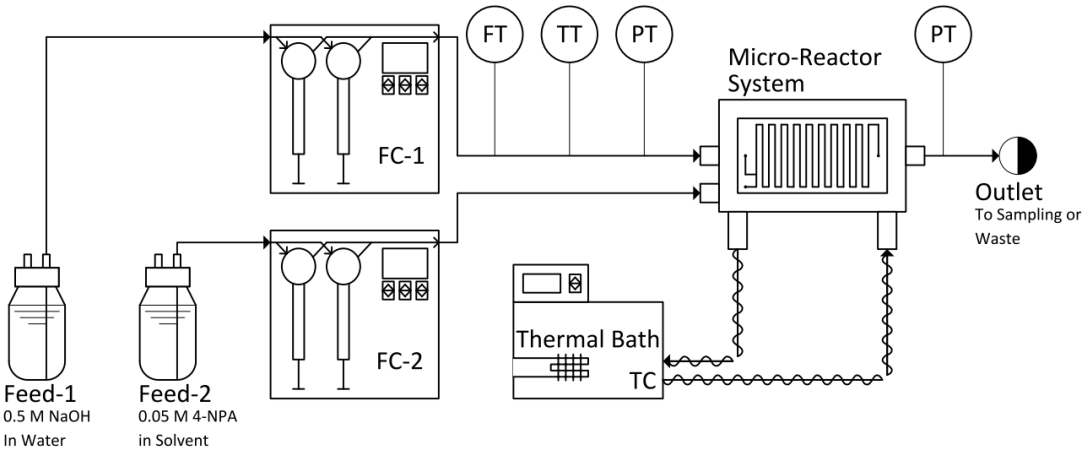

Figure 1.1. Typical continuous flow reactor experimental setup. Instruments identified are Flow Controllers (FC), Flow Transmitter (FT), Temperature Controller (TC), Temperature Transmitter (TT) and Pressure Transmitter (PT). Figure used from Plouffe, et al. [9]

Micro-reactors have typical channel width and height dimensions ranging from ~10 µm to 5,000 µm.[10] The miniature dimensions produce their distinctive high surface area-to-volume ratio (circa 10,000 m^2/m^3).[11,12] The incurred advantages allow process intensification[2] through: reducing the limitations in heat and mass transfer [4,5,13]; avoiding hot spots in highly exothermic reactions[14,15]; safely permitting highly hazardous reactions[3] [16–18]. The micro-reactor mixing is seen as an "emulsion generator"[19] when applied to immiscible liquid-liquid system and is classified into passive and active mixing mechanism.[20,21] Figure 1.2 shows a sub-classification of these, a part of both mechanisms are explored in this thesis and are explained in the following section along with the research objectives.

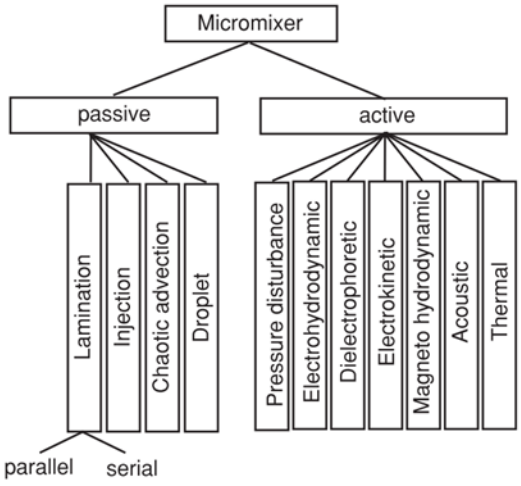

Figure 1.2. Classification of mixing mechanism in micro-reactors (Nguyen N-T. et Wu Z.) [10]

[2] Process intensification can be defined as "any chemical engineering development that leads to a substantially smaller, cleaner and more energy-efficient technology"[24].

[3] Hazardous reactions implicate elements such as hazardous reagents, toxic or explosive intermediates, or operating close to flash points.

1.2 Research Objectives

Passive mixing uses the kinetic energy provided by the upstream pump or pressure.[22] General examples of passive mixing in process engineering are: baffle plates in a reactor, in-line static mixers, trays in a distillation column, and packing material in a packed-bed reactor. At the micro-reactor scale, techniques such as Y- and T-junctions, split-and-recombine, 3D structures, twisted channels, and static mixing elements are used.[23] Many of these techniques such as different type of static mixing element geometry have previously been examined in order to evaluate interphase mass transfer rates.[13] The first topic in this thesis explores interphase mass transfer rates performance for various interspacing lengths between recently developed commercial mixing units. Interspacing is used to maximise the volume within a given plate reactor in order to ultimately achieve greater yields despite the resulting decrease in interphase mass transfer rates. There is thus geometrical optimisation.

Active mixing uses an external energy source other than the primary kinetic flow energy.[22] Examples of active mixing in process engineering are: agitator in a stirred-tank, recirculation pump in a tank, gas sparging in a tank, repulper in a pulp washer, fluidised bed, and screw mixer. Instances of active mixing used on the micro-reactor scale are: ultrasound, microwave, micro-stirrers, secondary pulsed flow, piezoelectrically vibrating membrane.[20] The second topic of this thesis is to explore the interphase mass transfer rates of secondary pulsed flow in a continuous flow coiled reactor. Research on an oscillatory-flow coil reactor without baffles is chosen since

much research has been completed in baffled tubes with little performance comparison to baffle-less tubes. The latter should better permit reactions where the product(s) is a solid (e.g., precipitation reactions), which is an important reaction class of the fine chemical and pharmaceutical industries for which passive mixing micro-reactor technology is not readily applicable due to channel plugging.

1.3 Thesis Outline

Section 2 examines the effect of channel length between mixing elements on interphase mass transfer rates in a bi-phasic liquid-liquid micro-reactor system. The results will be submitted for publication under the title "**Micro-Reactor Mixing Unit Interspacing for Fast Reactions in Liquid-Liquid Systems**". The two-phase alkaline hydrolysis of 4-nitrophenyl acetate (4-NPA) is used to determine the overall volumetric mass transfer coefficient as a function of the average rate of energy dissipation. Multiple solvent-pairs of immiscible bi-phasic media of water coupled with *n-butanol*, *n-hexanol-*, *Methyl tert-butyl ether* (*MTBE*), or *Toluene* are used to determine the applicability of a channel between mixing units.

Section 3 investigates the mixing efficiency of a secondary pulsed flow in a continuous flow coil reactor. It has been published under the title "**Liquid-Liquid Mass Transfer in an Oscillatory-Flow Mesoscale Coil Reactor without Baffles**". The overall volumetric mass transfer coefficients are evaluated with the two-phase alkaline hydrolysis of 4-NPA in a toluene−water system. An oscillatory-flow Reynolds number from 0 to 5,000 is used as secondary pulsed flow. The results are compared to different passive mixing micro-

reactor plates on the basis of energy dissipation rate in order to consider its proper usage in a toolbox approach[4].[22]

[4] The toolbox approach presented by Plouffe, et al. [22] is used to effectively select a reactor type by considering the mixed media (liquid-liquid, gas-liquid, homogeneous, etc.) and the rapidity of the reaction.

1.4 References

[1] López-Guajardo, E., Ortiz-Nadal, E., Montesinos-Castellanos, A., and Nigam, K. D. P., 2017, "Coiled Flow Inverter as a Novel Alternative for the Intensification of a Liquid-Liquid Reaction," Chem. Eng. Sci., **169**, pp. 179–185.

[2] Phan, A. N., Harvey, A. P., and Eze, V., 2012, "Rapid Production of Biodiesel in Mesoscale Oscillatory Baffled Reactors," Chem. Eng. Technol., **35**, pp. 1214–1220.

[3] Zheng, M., Skelton, R. L., and Mackley, M. R., 2007, "Biodiesel Reaction Screening Using Oscillatory Flow Meso Reactors," Process Saf. Environ. Prot., **85**, pp. 365–371.

[4] Ueno, M., Hisamoto, H., Kitamori, T., and Kobayashi, S., 2003, "Phase-Transfer Alkylation Reactions Using Microreactors," Chem. Commun., (8), pp. 936–937.

[5] Kashid, M. N., and Kiwi-Minsker, L., 2009, "Microstructured Reactors for Multiphase Reactions: State of the Art," Ind. Eng. Chem. Res., **48**(14), pp. 6465–6485.

[6] Administration, U. S. F. and D., 2017, "The Drug Development Process" [Online]. Available: https://www.fda.gov/forpatients/approvals/drugs/ucm405622.htm.

[7] Kane, A., 2016, "Phase-Appropriate Formulation and Process Design," Pharm. Technol., **40**(1).

[8] Hay, M., Thomas, D. W., Craighead, J. L., Economides, C., and Rosenthal, J., 2014, "Clinical Development Success Rates for Investigational Drugs," Nat. Biotechnol., **32**(1), pp. 40–51.

[9] Plouffe, P., Bittel, M., Sieber, J., Roberge, D. M., and Macchi, A., 2016, "On the Scale-up of Micro-Reactors for Liquid-Liquid Reactions," Chem. Eng. Sci., **143**, pp. 216–225.

[10] Nguyen, N.-T., and Wu, Z., 2005, "Micromixers — A Review," J. Micromech. Microeng., **15**, pp. R1–R16.

[11] Fogler, H. S., 2006, "Elements of Chemical Reaction Engineering," Prentice Hall PTR Int. Ser. Phys. Chem. Eng. Sci., **4th**, p. 201.

[12] Plouffe, P., 2015, "Micro-Reactor Design for Fast Liquid- Liquid Reactions," (PhD thesis) University of Ottawa.

[13] Plouffe, P., Macchi, A., and Donaldson, A. A., 2013, "Enhancement of Interphase Transport in Mini-/Microscale Applications Using Passive Mixing," Heat Transf. Eng., **34**, pp. 159–168.

[14] Plouffe, P., Roberge, D. M., and Macchi, A., 2015, "Liquid-Liquid Flow Regimes and Mass Transfer in Various Micro-Reactors," Chem. Eng. J., p. 10 pp.

[15] Mielke, B. E., 2017, "Study on the Transport Phenomena in Complex Micro-Reactors." (Master's thesis) University of Ottawa

[16] Schneider, M. A., and Stoessel, F., 2005, "Determination of the Kinetic Parameters of Fast Exothermal Reactions Using a Novel Microreactor-Based Calorimeter," Chem. Eng. J.,

115(1–2), pp. 73–83.

[17] Yoshida, J., 2008, *Flash Chemistry: Fast Organic Synthesis in Microsystems*, Wiley.

[18] Ducry, L., and Roberge, D. M., 2005, "Controlled Autocatalytic Nitration of Phenol in a Microreactor," Angew. Chemie - Int. Ed., **44**(48), pp. 7972–7975.

[19] Kockmann, N., and Roberge, D. M., 2011, "Scale-up Concept for Modular Microstructured Reactors Based on Mixing, Heat Transfer, and Reactor Safety," Chem. Eng. Process. Process Intensif., **50**(10), pp. 1017–1026.

[20] VandenBussche, K. M., 2007, *Micro Instrumentation : For High Throughput Experimentation and Process Intensification - a Tool for PAT*, Wiley-VCH, Weinheim.

[21] Hessel, V., Löwe, H., and Schönfeld, F., 2005, "Micromixers - A Review on Passive and Active Mixing Principles," Chem. Eng. Sci., **60**(8–9 SPEC. ISS.), pp. 2479–2501.

[22] Steinke, M. E., and Kandlikar, S. G., 2004, "Review of Single-Phase Heat Transfer Enhancement Techniques for Application in Microchannels, Minichannels and Microdevices," Int. J. Heat Technol., **22**(2), pp. 3–11.

[23] Plouffe, P., Macchi, A., and Roberge, D. M., 2014, "From Batch to Continuous Chemical Synthesis - A Toolbox Approach," Org. Process Res. Dev., **18**, pp. 1286–1294.

[24] Lee, C. Y., Wang, W. T., Liu, C. C., and Fu, L. M., 2016, "Passive Mixers in Microfluidic Systems: A Review," Chem. Eng. J., **288**, pp. 146–160.

[25] Stankiewicz, A. I., and Moulijn, J. A., 2000, "Process Intensification: Transforming Chemical Engineering," Chem. Eng. Prog., **96**(1), pp. 22–34.

2 Micro-Reactor Mixing Unit Interspacing for Fast Reactions in Liquid-Liquid Systems

Eric Mielke,[a] Sébastien S. Mongeon,[a] Christof Aellig,[b] Sarah Filliger,[b] Patrick Plouffe,[a] Arturo Macchi,[a] and Dominique M. Roberge[b]

a, Centre for Catalysis Research and Innovation, Department of Chemical and Biological Engineering, University of Ottawa, K1N 6N5 Ottawa, Canada.

b, Chemical Manufacturing Technologies, Lonza AG, CH-3930 Visp, Switzerland.

This manuscript will be submitted for publication in 2017

ABSTRACT

The effect of geometrical arrangements of a residence time channel between mixing elements on interphase mass transfer rates is investigated. Four variations of a micro-reactor plate using LL-Rhombus static mixing elements with a contraction size of 500 µm by 1,250 µm are tested with immiscible aqueous-organic systems varying from 1.8 mN/m to 35.4 mN/m in interfacial tension. The bi-phasic systems are water coupled with *n-butanol*, *n-hexanol*, *Methyl tert-butyl ether* (MTBE), and *Toluene*. The two-phase alkaline hydrolysis of 4-nitrophenyl acetate (4-NPA) is used to determine the overall volumetric mass transfer coefficient. Although there is an impact of the geometrical arrangement of residence time channel, the greatest driver on interphase mass transfer rates is the ratio of the volume of residence time channels to number of mixing units. An algorithm for selecting optimal reactor operating conditions is given.

2.1 Introduction

2.1.1 Micro-Reactor Design

Many fine chemicals and pharmaceuticals are manufactured by solvent-intensive batch or semi-batch processes with high costs and environmental impact.[1] In comparison, continuous-flow micro-reactors offer a high surface-to-volume ratio and intimate contact between reactants, which leads to rapid heat and mass transfer that improve reaction control and selectivity. This, coupled with their small volume, proactively makes the handling of hazardous reactions and unstable intermediates more safe and efficient. Micro-reactors can be modular to provide different, well-controlled (i.e., rapid dynamic response), process conditions and residences times. This approach ultimately facilitates scale-up once optimal process configuration and operating conditions are identified. Altogether, micro-reactors intensify the process with enhanced transport phenomena that allow for more severe conditions relative to batch reactors.

There are still challenges for the wider use of micro-reactor systems; a significant issue is the lack of information for different operating conditions to obtain good and predictable reactor performance. Understanding the micro-reactor performance through multiple operating conditions and configurations such as the channel length between mixing units will lead to a more systematic and effective choice in reactor design. This facilitates migrations of batch to continuous processes through the use of the micro-reactor.

For this reason, Plouffe et al. [1] developed a “toolbox” to help select a reactor type effectively. Reactive systems were divided into reaction types based on their kinetics/thermal requirements, as well as the phase(s) involved (homogenous, liquid-liquid, liquid-gas, gas-solid, etc.). For fast reactions in immiscible liquid-liquid systems, the LL-Rhombus mixer (Figure 2.1) was shown to be an effective tool for achieving the drop flow regime at relatively low energy dissipation rates,[2,3] allowing for higher rates of interphase mass transfer due to increased specific area compared with other flow regimes (e.g., slug/parallel flow). The mixing unit is designed with specific properties: a sudden curved expansion to create mixing while reducing dead zones; a rhomboid obstacle to split the flow in order to utilise the unit volume and avoid jetting at the centre; a gradual contraction in order to minimize the pressure drop to the contraction.

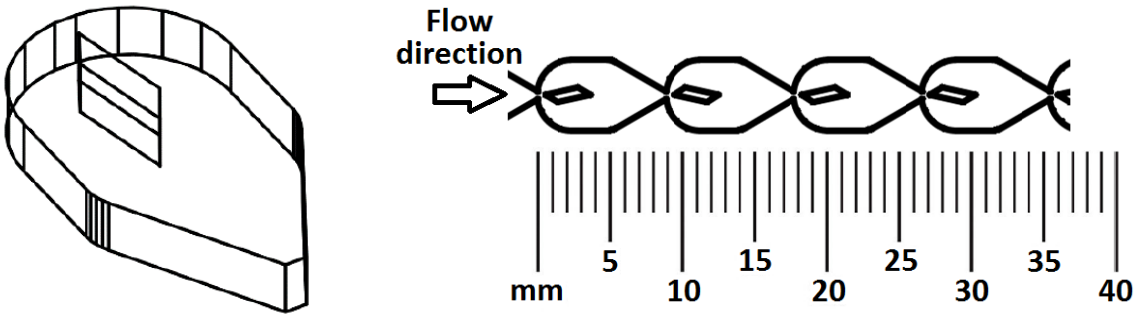

Figure 2.1. 3D representation (left) and linear sequencing (right) of the LL-Rhombus mixing unit.

The purpose of this work is to investigate the effect of mixing unit interspacing on the performance of a liquid-liquid system micro-reactor. Characterising the impact of the interspacing will allow for the optimisation of the geometrical design of the micro-reactor for various operating conditions. While having the highest rates of mass transfer is useful in fully mass-transfer limited systems, determining an optimal space between

mixers for different solvent pairs could maximise the total production rate of a chemical and minimise energy consumption (i.e., pressure drop) simultaneously.

To characterise the impact of spacing between mixing units, the following performance parameters will be evaluated: pressure drop, average energy dissipation rate, test reaction conversion, and overall interphase volumetric mass transfer coefficient. These parameters are interrelated such that the fluid dynamics are affected by the reactor designed geometry and operating conditions.

2.2 Experimental

2.2.1 Selected Micro-Reactor Designs

Four micro-reactor plates of size A5 (148 mm x 210 mm) were manufactured using the LL-Rhombus as the base mixing unit and interspaced by residence time channels (RTC) of different lengths. The various spacing setups are illustrated in Figure 2.2, and the properties are in Table 2.1 and

Table 2.2.

Table 2.1. Micro-Reactor Plate Properties[5]

micro-reactor name	mixing unit arrangement	number of mixing units	total plate volume [mL]
continuously mixed	xxxxxx	223	10.3
grouped	xxx===	86	18.8
equally spaced	x=x=x=	86	19.5
minimal	x=====	46	22.2

[5] Only the second half of the micro-reactors' volumes were used for n-Butanol-water systems to avoid conversion close to 100% before exit.

Table 2.2. Size 300 LL-Rhombus Mixer and RTC Cross-Sectional Dimensions

parameter	value	[units]	value	[units]
contraction size	**mixing unit**		**RTC region**	
W	0.500	[mm]	5.00	[mm]
L	1.250	[mm]	2.00	[mm]
d_h	0.714	[mm]	2.86	[mm]
volume per mixer	0.046	[mL]		

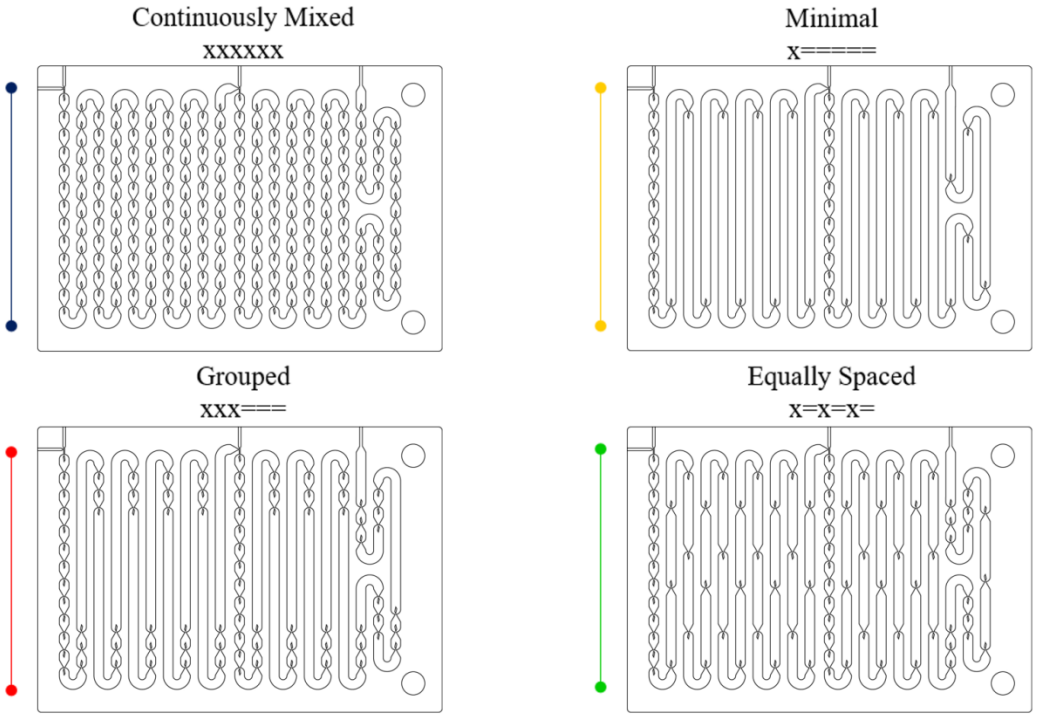

Figure 2.2. 2D CAD of the A5 (148 mm x 210 mm) micro-reactor plates with varied mixer spacings.

The location of the mixers in the “grouped” and “minimal” spaced micro-reactors were placed after the bends in the residence time channel due to potential phase separation observed in curved channels from centrifugal forces.[2]

2.2.2 Test Reaction for Interphase Mass Transfer in Different Solvents

The selected reaction to perform the interphase mass transfer tests is the alkaline hydrolysis of 4-nitrophenyl acetate (4-NPA), shown in Figure 2.3. This reaction is

dependent on interphase mass transfer rather than reaction kinetics as the corresponding reaction kinetic rate constant of 14 L/mol/s [4 - 6] is very high.

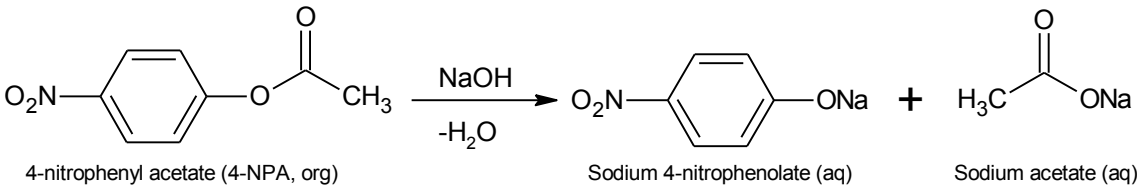

Figure 2.3. Alkaline hydrolysis of 4-nitrophenyl acetate.[2]

The 4-NPA is nearly exclusively soluble in the organic phase with a solubility of less than 2.5 mmol/L in water at 23 °C. The organic phase was a 0.05 mol/L solution of the acetate in either *n-butanol*, *n-hexanol*, *methyl tert-butyl ether* (MTBE) or *toluene*. These solvents were chosen due to their distinct physical properties, see Table 2.3 as reported from Plouffe et al.[7] The NaOH is dissolved in the aqueous phase and fed at the same volumetric flow rate as the organic phase such to have a molar ratio of 10:1 with the 4-NPA. This ensures that the reaction is pseudo-first order since the full conversion and neutralisation of the phenyl and acetate group ratio requires only a 2:1 stoichiometric ratio.

Table 2.3. Physical and thermodynamic properties of solvents at ambient temperature (23°C).[7]

solvent	**σ (mN/m)**	**ρ (kg/m^3)**	**μ (mPa·s)**	**H_A (-)**	**D_A (m^2/s)**
n-Butanol	1.8	806	2.6	31 ± 2	3.6E-10
n-Hexanol	6.6	815	4.5	40 ± 7	2.3E-10
MTBE	10.5	737	0.4	115 ± 24	25E-10
toluene	35.4	862	0.6	230 ± 7	17E-10
0.5 M NaOH in water	-	1020	1.1	-	6.1E-10

The reaction samples were collected directly into a quench solution of acetonitrile, water, and acetic acid. The acetic acid reacts with the NaOH in the aqueous phase to stop the hydrolysis 4-nitrophenyl acetate reaction. The molar ratio of acetic acid to NaOH was set to 6 to 1. The quench solution compositions for the different liquid-liquid systems are shown in Table 2.4. For Toluene and MTBE, a lower concentration of acetic acid was required to maintain a homogenous overall quench mixture.

Table 2.4. Quenching solution for the hydrolysis of 4-nitrophenyl acetate.

	toluene [% w/w]	**n-butanol [% w/w]**	**MTBE [% w/w]**	**n-hexanol [% w/w]**
acetonitrile	72.8	72.0	72.8	72.0
water	26.5	26.2	26.5	26.2
acetic acid	0.7	1.8	0.7	1.8

The samples were analysed with an HP Agilent 1100 series HPLC system with a 250 mm × 4.6 mm i.d. Agilent Zorbax SB-C8 at room temperature. Using the obtained conversion of 4-NPA (η), the overall volumetric mass transfer coefficient ($K_{org}a$) can be determined by performing a plug flow mass balance over a control volume of the dispersed phase and integrating over the reactor residence time as presented in equation (2.1) where (ϕ) is the volumetric phase fraction and (τ) is the average fluid residence time.[2,7,8] The fluid-fluid systems use the entire reactor volumes, except for the *n-butanol-water* where only half of each reactor is used in order to limit conversion to below 100% at the exit.

$$K_{org}a = -\frac{\phi}{\tau}\ln(1-\eta) \tag{2.1}$$

2.3 Results

2.3.1 Pressure Drop

The two-phase pressure drop for each micro-reactor was measured for total flow rates ranging up to 180 mL/min; with the *toluene-water* and *n-butanol-water* systems results shown in Figure 2.4. The pressure drop from the "grouped" and "equally spaced" micro-reactors (each with three mixing units per row arrangement) show similar values for a given solvent pair. The pressure drop of the "continuously mixed" micro-reactor is the highest while the "minimal" spaced micro-reactor with a single unit per row is the lowest.

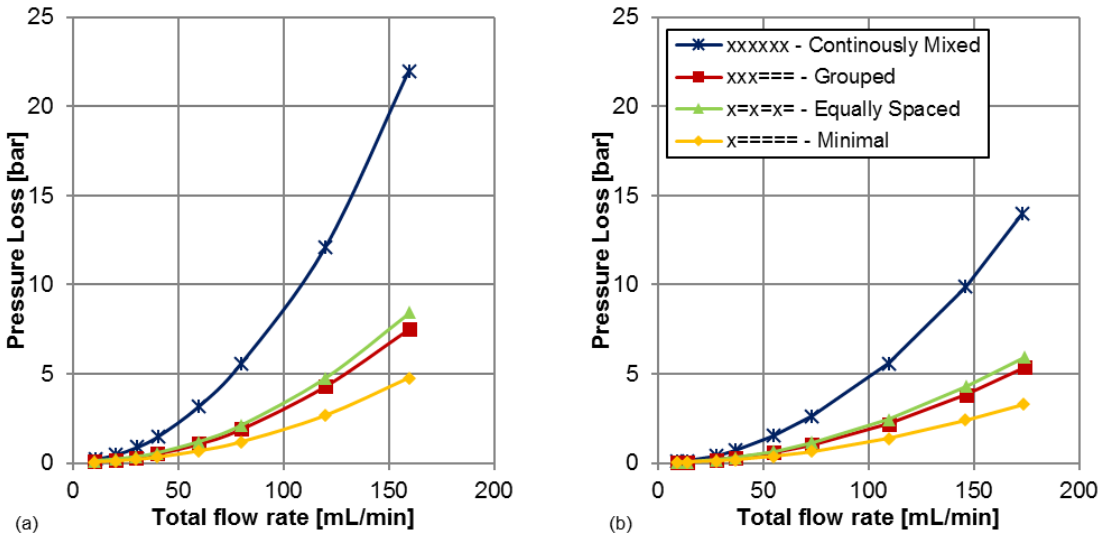

Figure 2.4. Pressure drop vs. total flow rate of each micro-reactor:
(a) *toluene-water* with full reactor volumes and (b) *n-butanol-water* with half reactor volumes

The pressure losses from the four micro-reactors are also compared on a mixing unit basis in Figure 2.5 for both solvent pairs. The results show that every micro-reactor follows the same non-linear trend independently of the mixing unit arrangement that

was chosen. This means that the change in channel geometry caused by the addition of the RTC did not significantly contribute to an increase in pressure loss and the majority of the energy is dissipated in the mixing unit regions of the micro-reactors.

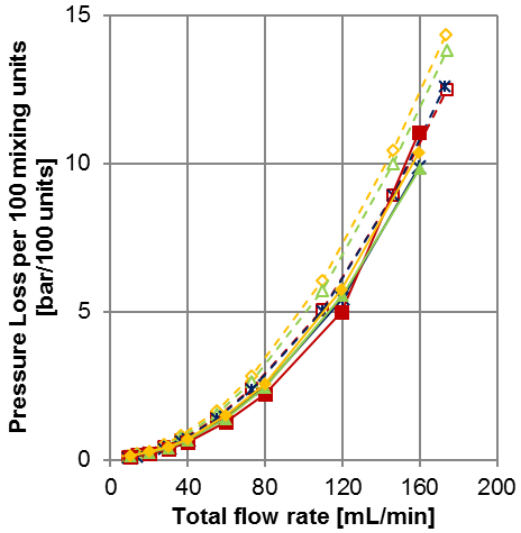

Figure 2.5. Pressure loss per 100 mixing units vs. total flow rate of each micro-reactor with *toluene-water* (solid lines) and *n-butanol-water* (dashed lines, empty symbols) using the same legend as Figure 2.4

2.3.2 Flow Regime Analysis: Conversion vs Total Flow Rate

The first comparison of the mass transfer for a given reactor uses the reaction conversion vs. flow rate. For the "continuously mixed" micro-reactor, it is possible to directly compare the flow regimes observed for the *toluene-water* and *n-butanol-water* systems with those in previous work in the FlowPlate® Lab reactor,[3] which allows visual inspection/pictures. It was previously observed that the LL-Rhombus size 300 had a transitionary flow regime with the presence of both larger slugs (or elongated drops) and smaller spherical drops up to total flow rates of 20 and 50 mL/min for *n-butanol-water* and *toluene-water* systems, respectively. Any higher flow rate yielded the drop flow regime with spherical drops significantly smaller than the channel diameter. The

"continuously mixed" micro-reactor results from Figure 2.6 (a) and (b) agree with the expected flow regimes. The conversion is increasing with flow rate until the flow regime is no longer transitioning, and reaches drop flow. The interfacial area available for mass transfer continues to increase with flow rate (due to smaller and more numerous drops); however, once the flow regime is steady, the decrease in residence time with flow rate has a stronger impact on the total mass transferred. It is reasonable to conclude that the same effect is occurring with *MTBE* and *n-hexanol* in the "continuously mixed" micro-reactor, where drop flow is determined to be achieved by 20 mL/min for *MTBE-water* and 40 mL/min for n-hexanol.

From the results in Figure 2.6, the onset of the drop flow regime is estimated for the other three micro-reactors by the flow rate at which the decrease in conversion becomes a monotonic function. These estimated flow rates are presented in Table 2.5. For a given geometry, the drop flow regime occurs first with the *MTBE* due to a combined relatively low interfacial tension and viscosity, then with the *n-butanol, n-hexanol and toluene*. Lower viscosity and interfacial tension facilitate the formation on interfacial area when energy is dissipated within the system. These results also corroborate with the findings of Plouffe et al. [7] using a serpentine channel geometry.

Table 2.5. Estimated flow rate (in [mL/min]) required for the onset of the drop flow regime in the studied reactors and solvent systems.[6]

	continuously mixed **xxxxxx**	**equally spaced** **x=x=x=**	**grouped** **xxx===**	**minimal** **x=====**
toluene-water	**50**	120	120	≥160
n-hexanol-water	40	60	80	80
n-butanol-water	**20**	60	80	120
MTBE-water	20	40	60	60

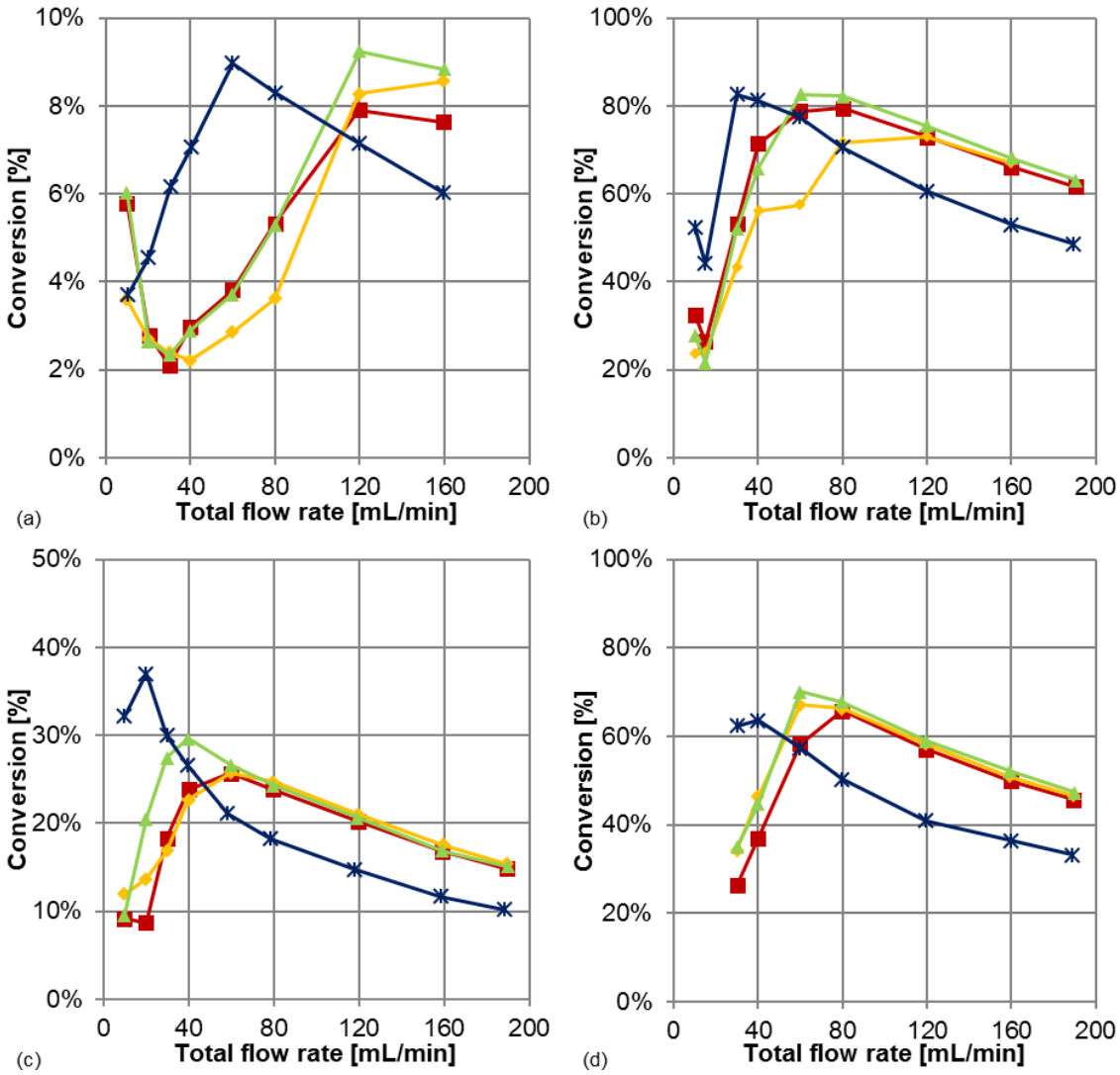

Figure 2.6. Conversion vs. total flow rate for each micro-reactor (same legend as Figure 2.4): (a) *toluene-water*; (b) *n-butanol-water*; (c) *MTBE-water*; and (d) *n-hexanol-water systems*

[6] Bold values indicate results observed visually in Mielke et al. [3]

Considering first the case with *toluene-water,* the solvent pair with the highest interfacial tension (σ), the drop flow regime occurred earliest with the "continuously mixed" micro-reactor, as clearly shown by the earliest peak in conversion vs. flow rate. The "minimal" spaced micro-reactor on the other hand requires a much greater flow rate for generating stable drops throughout the entire reactor volume, which was not conclusively observed, even at 150 mL/min. While drops may form in a given mixing unit in each micro-reactor, they likely re-coalesce in the RTC until the residence time is sufficiently short that coalescence becomes negligible. The "grouped" and "equally spaced" micro-reactors present similar performances across the range of flow rates. Finally, when each micro-reactor is in the same flow regime, the increased residence time becomes advantageous for conversion, since the micro-reactors with spacing between the mixers have over double the reactive volume compared to the "continuously mixed" micro-reactor.

Considering then the case with the lowest σ, *n-butanol-water*, similar relationships between the "continuously mixed" and "minimal" spaced micro-reactors were observed; although the relative conversion differences between these two micro-reactors are lower. Indeed, the flow rates required to reach the drop flow regime are much lower for all micro-reactors in addition to the overall conversions being much greater due to the decreased σ and increased solubility of *n-butanol* in water. The "grouped" and "equally spaced" micro-reactors again present similar performances across the range of flow rates.

The intermediate solvent systems, *MTBE-water* and *n-hexanol-water* (with σ between those of *toluene-water* and *n-butanol-water*), gave results similar results to *n-butanol-water*, except with lower conversions primarily due to greater interfacial tension and lower solubility. For all solvent pairs, "continuously mixed" micro-reactors entered the drop flow regime at lower flow rates than the other mixer spacing arrangements.

2.3.3 Conversion and Rate of Interphase Mass Transfer vs Rate of Energy Dissipation

In order to compare the various micro-reactor arrangements, it is useful to use the average energy dissipation rate, ε, defined in equation (2.2), rather than the total flow rate. This normalises the results, taking into account the different pressure drops and reactor volumes for each mixer spacing configuration.

$$\varepsilon = \frac{\Delta P Q}{\rho_c V_R} = \frac{\Delta P}{\rho_c \tau} \tag{2.2}$$

The conversion is plotted versus ε for each solvent in Figure 2.7. While the "continuously mixed" micro-reactor generally outperforms the configurations with spacing for samples at lower ε, it is difficult to draw further conclusions from the low ε results due to the potentially stochastic variations in this transitionary slug/drop flow regime.[3] Interestingly, the maximum conversion for each mixer spacing still occurs at similar range of ε for a given solvent pair. At the point of maximum conversion, an increase in energy dissipation rate results in a lower residence time, τ, negating the

benefits of increased overall mass transfer rates. For this reason, regardless of reactor selection or solvent system, it is desirable to operate at the average energy dissipation rate that corresponds to the onset of the drop flow regime, ε^*, to achieve the maximum conversion in a reactor.

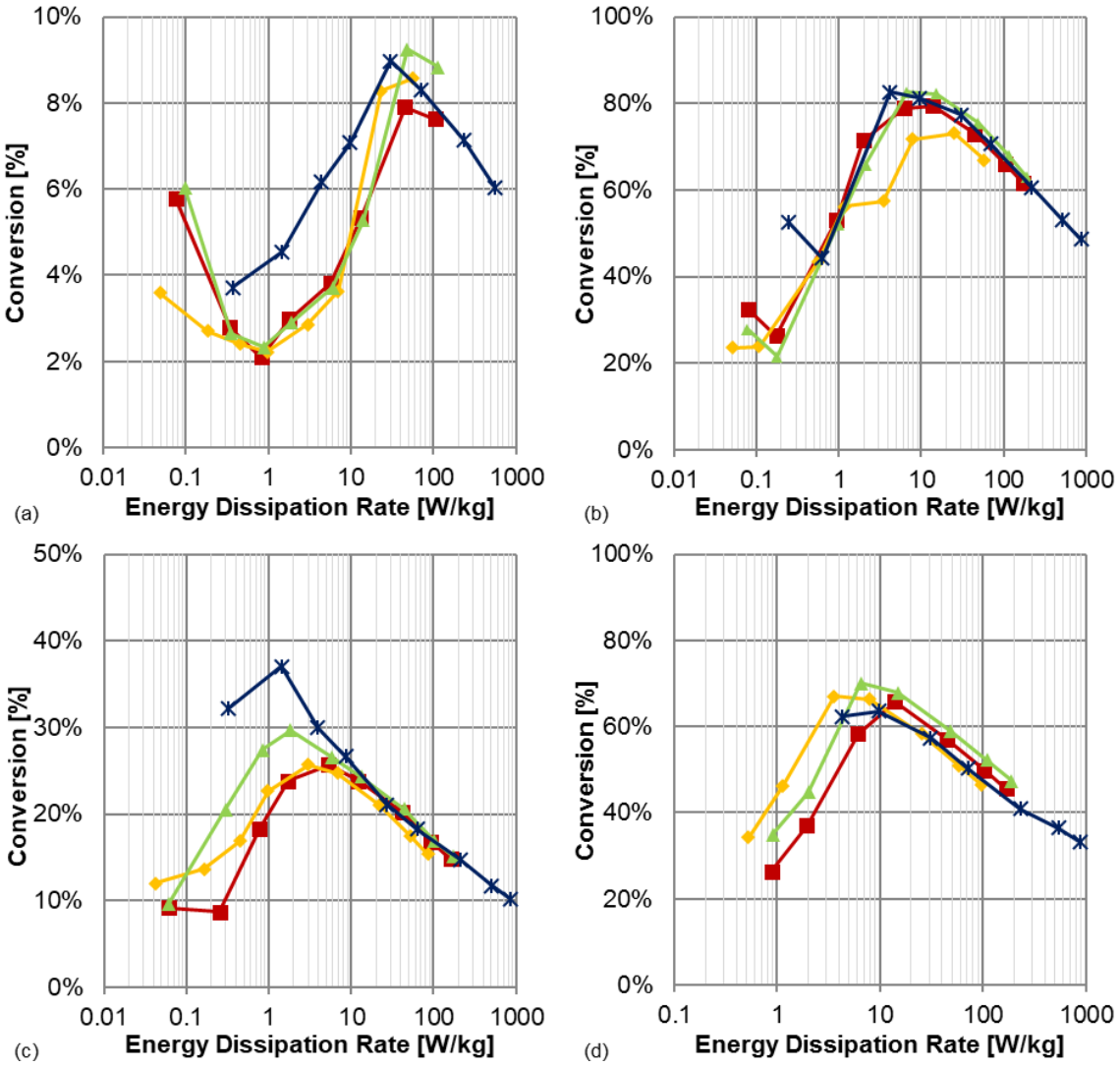

Figure 2.7. Conversion vs. average rate of energy dissipation for each micro-reactor (same legend as Figure 2.4): (a) *toluene-water*; (b) *n-butanol-water*; (c) *MTBE-water*; and (d) *n-hexanol-water* systems

The overall volumetric mass transfer coefficient normalises the conversion between reactors on a residence time basis. Figure 2.8 shows $K_{org}a$ vs energy dissipation rate for

all data points in the drop flow regime (those highlighted in Table 2.5) for every micro-reactor plate and solvent pair studied here. Although the energy dissipation rate at the onset of drop flow, ε^*, was similar for the different reactors, it is still generally lowest for the "continuously mixed" design. Once the system achieved the drop flow regime, $K_{org}a$ was no longer a function of channel geometry, but rather the rate of energy dissipation and the phase physical properties.[2, 3] These results also suggest that, until the drop flow regime is reached, droplets formed in the mixers likely coalesced in the RTC and that advective mass transfer was significantly reduced. For a given flowrate, in the established drop flow regime, it was originally hypothesised that a dispersion generated by several mixing units could be sustained in the RTC section; which would then likely increase the $K_{org}a$ for a lower ε requirement from the possibility of diffusional effect in the small drops but obviously the drops are still too large to account for this effect. To achieve this objective, minimising curvature would be essential to avoid re-coalescence.[2] This was the basic design strategy of the "minimal" micro-reactor where a dispersion was re-created after each individual curve (except in the entrance region). Ultimately, unless the energy dissipation rate is sufficient to maintain drop flow in the RTC, the "continuously mixed" micro-reactor will provide the better performance.

The $K_{org}a$ of each solvent pair from Figure 2.8 was fit to equation (2.3)(2.1) with the parameters and the 95% confidence intervals shown in Table 2.6. The pre-exponential value is a function of the solvent-pair and positively trends with conditions conducive to interface creation upon energy dissipation (e.g., low interfacial tension) and have

greater miscibility with water. The exponential factors for all four solvent-pairs were similar as also visually observed by the slopes.

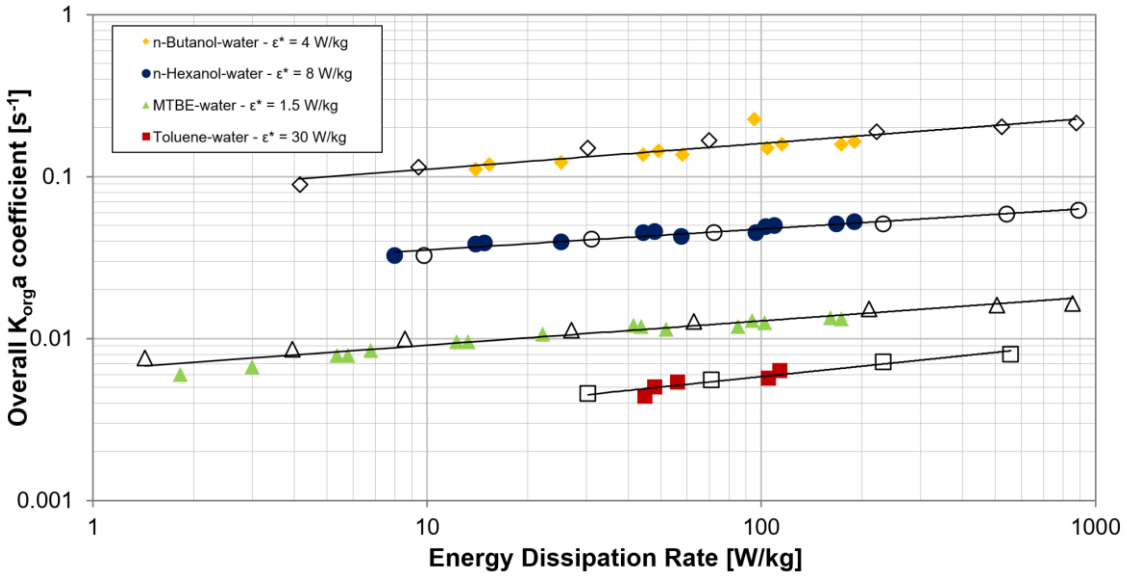

Figure 2.8. $K_{org}a$ vs. $\boldsymbol{\varepsilon}$ for all data points in the drop flow regime for each micro-reactor for various solvents. Points from the "continuously mixed" micro-reactor are highlighted by the open symbols. $\boldsymbol{\varepsilon}^*$ refers to the energy dissipation rate at the onset of drop flow for a given organic-aqueous solvent pair.

$$\left(K_{org}a\right)_{modeled} = \alpha\ \varepsilon^{\beta} = -\frac{\phi}{\tau}\ln(1-\eta) \tag{2.3}$$

Table 2.6. Model parameters for equation (2.3) with a 95% confidence interval for each solvent pair.

solvent pair	$\boldsymbol{ln(\alpha)}$	$\boldsymbol{\beta}$
n-butanol-water	-2.6 ± 0.2	0.16 ± 0.04
n-hexanol-water	-3.64 ± 0.07	0.13 ± 0.02
MTBE-water	-5.04 ± 0.06	0.15 ± 0.02
toluene-water	-6.1 ± 0.2	0.21 ± 0.05

2.4 Discussion

2.4.1 Practical Implications of Operation above $\boldsymbol{\varepsilon^*}$ and Solvent Selection

To demonstrate the required pressure drop for a given conversion, Figure 2.9 was generated for *toluene-water* and *n-butanol-water* by rearranging equations (2.1), (2.2), and (2.3) for a given solvent into equation (2.4);. additionally, the pressure drop vs. ε is plotted for various residence times using only equation (2.2). The intersection of a given conversion and residence time curve indicates the required pressure drop to achieve those conditions. The benefit of operating at the lowest ε that yields drop flow, ε^*, becomes clear.

$$\Delta P = -\frac{\phi \varepsilon \rho_c}{\alpha \varepsilon^{\beta}} \ln(1-\eta) \tag{2.4}$$

$$\Delta P = -\frac{\phi \varepsilon^{1-\beta} \rho_c}{\alpha} \ln(1-\eta)$$

Note that due to the poor rates of interphase mass transfer in the *toluene-water* system, large pressure drops (over 8 bar) and long residence times are required to achieve conversions over 20%. This contrasts *n-butanol-water*, where 80% conversion is obtained at pressure drops below 1 bar due to the lower interfacial tension, higher miscibility, as well as the onset of the drop flow regime at a lower ε. This effect can be observed in Figure 2.10, which plots the pressure drop as a function of conversion from equation (2.4) (holding ε constant). While at equivalent energy dissipation rates, *n-*

hexanol may seem like a better option than *MTBE* (Figure 2.10a), but due to the early onset of drop flow for MTBE-water, the same pressure drops are required for equivalent conversions when operating at the onset of drop flow for both systems (Figure 2.10b).

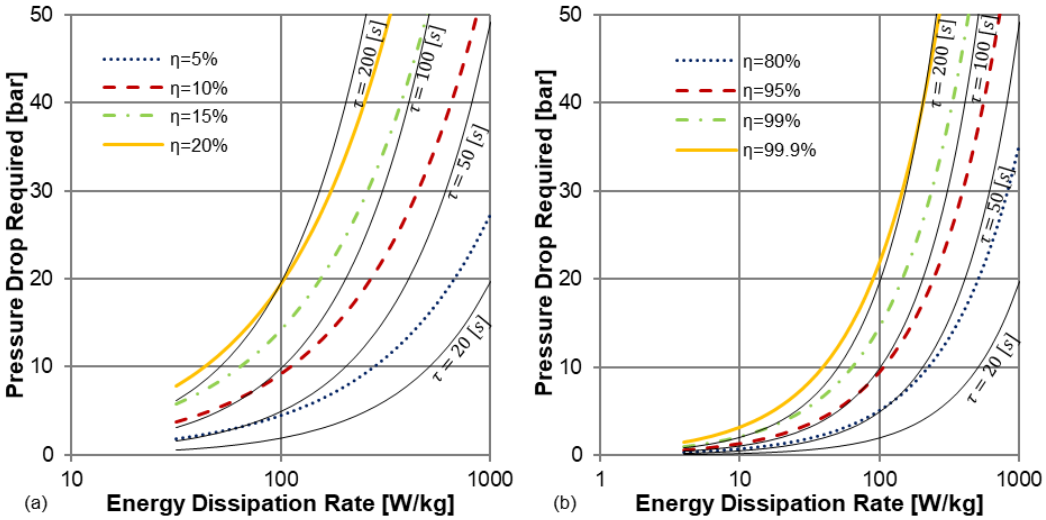

Figure 2.9. Pressure drop required to achieve a given conversion at a given $\boldsymbol{\varepsilon}$, and τ (solid black lines): (a) toluene-water and (b) n-butanol-water

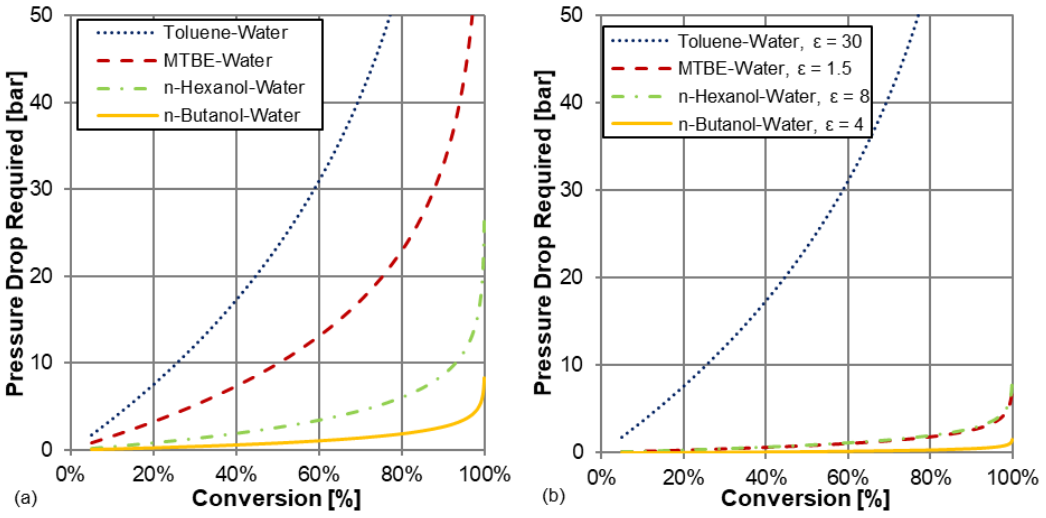

Figure 2.10. Pressure Drop vs. Conversion for each solvent system at (a) $\boldsymbol{\varepsilon}$ = 30 W/kg and (b) the minimum $\boldsymbol{\varepsilon}$ required for drop flow, $\boldsymbol{\varepsilon}^*$ in [W/Kg]

2.4.2 Algorithm for the Optimal Selection of a Reactor

For any liquid-liquid reaction to be performed under a plug flow pattern in the proposed mixer, the size and volume of the reactor can be determined accordingly for a general case:

1. Choose a solvent system (or several) that is suitable for the application for initial screening. Solvent pairs with lower interfacial tensions decrease the reactor geometric requirements but can make downstream separation more difficult.
2. Perform the reaction in a test reactor across several flow rates while measuring pressure drop, ideally in a system where the flow regime can be observed such as in the FlowPlate® Lab and which has a smaller volume to limit material consumption. Identify the energy dissipation rate where drop flow occurs, ε^* (as in Figure 2.11). If the reaction is mass transfer limited, this should correspond with a maximum in conversion as well. The corresponding overall volumetric mass transfer coefficient, $K_{org}a^*$, can be calculated with these tests at ε^*.
3. With $K_{org}a^*$, calculate the required residence time, τ^*, to achieve the desired conversion with equation (2.1). The same process used to generate the curves in Figure 2.9 can be applied to calculate the required pressure drop for that residence time at ε^*. If this pressure drop is too large, the desired conversion can be reduced, or another solvent pair with better overall interphase mass transfer must be selected (as shown in Figure 2.10b). Alternatively, active mixing

technologies could be considered, such as pulsating-flow coil reactors,[9] to dissipate energy and create interfacial area in a reactor.

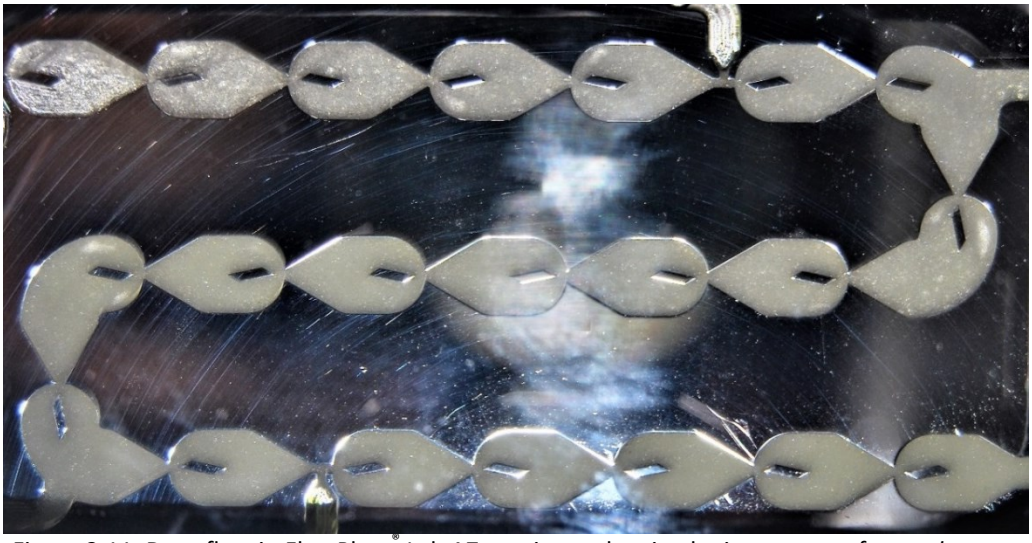

Figure 2.11. Drop flow in FlowPlate® Lab A7 continuously mixed micro-reactor for a *toluene-water* system.

4. If the pressure drop is acceptable, the flow rate (and thus production rate) must be selected. If there are several micro-reactor configurations in consideration (such as various scales or mixer spacings), test the energy dissipation rate (i.e., pressure drop) across different flow rates in two-phase flow, and determine the flow rates required for ε^*, as done for *toluene-water* and *n-butanol-water* in Figure 2.12. Select the reactor that achieves ε^* at a desired flow rate.

   Note that the grouped and equally spaced micro-reactors achieve the same ε for a given flow rate, as expected, since they have the same number of mixing units for a similar total volume.

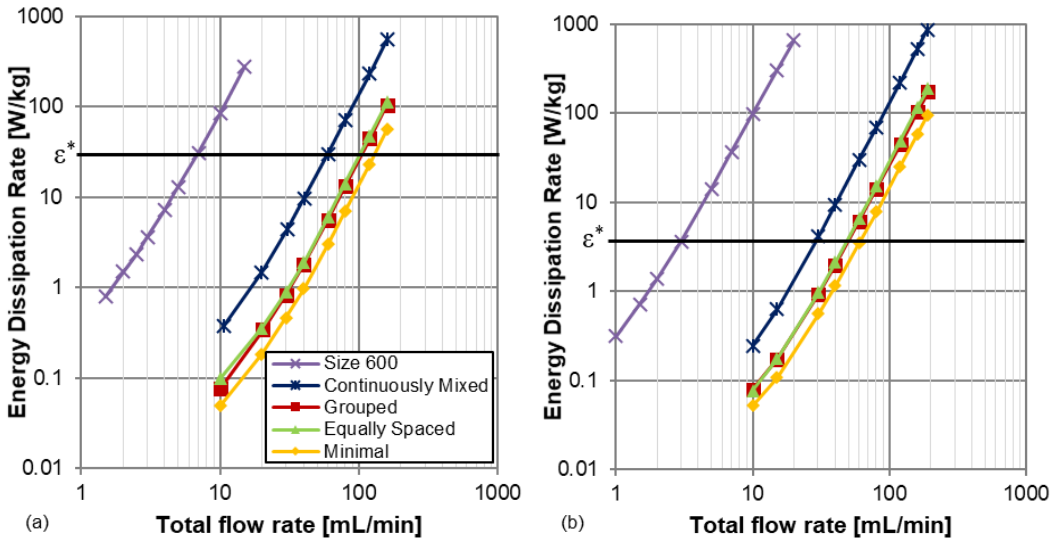

Figure 2.12. ε vs. total flow rate for each micro-reactor studied in addition to the size 600 "continuously mixed" micro-reactor (dh = 286 µm) in the (a) *toluene-water* and (b) *n-butanol-water* systems

5. Finally, determine the total micro-reactor volume required to achieve τ^* at the selected flow rate from the previous step. For a plate type reactor, it may mean to increase the plate length and height (area) or adding more plates in series by maintaining the internal structure at the same scale.

For the solvent systems studied in this work and the LL-Rhombus reactors, no further experimentation would be required to find the optimal reactor for a given production rate. The previous methods illustrate how to perform this analysis for any other of solvent pair to determine the optimal operating conditions. If the reaction under consideration is significantly endo/exothermic, this must also be taken into account when choosing the mixer scale to avoid hot-spot formation; though this will rarely become an issue with mass-transfer-limited liquid-liquid reactions.[10]

2.5 Conclusions

In order to determine the most efficient operating reactor design, several LL-Rhombus micro-reactors for the FlowPlate® system were manufactured with different spacing arrangements between the mixing-units. The two-phase alkaline hydrolysis of 4-nitrophenyl acetate was employed to analytically compare the mass transfer-limited systems of *toluene-water*, *n-butanol-water*, *MTBE-water*, and *n-hexanol-water* in each micro-reactor. Maximum conversion occurred at the onset of the drop flow regime for all operating conditions. For a given solvent pair, although the drop flow regime was achieved at similar ε for the different micro-reactor plates, it generally still occurred first with the "continuously mixed" design suggesting that droplets re-coalesce in the RTC. The two micro-reactors with different spacing arrangements, but the same number of mixing-units, did not yield significantly different results, which suggest that the ratio of mixing-unit to RTC volume plays a more important role.

The impact of operating at higher rates of energy dissipation than required for the onset of drop flow (ε^*) was investigated in terms of required pressure drop to achieve a certain conversion or residence time. The benefit of operating as close to ε^* as possible was demonstrated due to reduction of residence time negating the increase in the rate of mass transfer once drop flow is established. Lastly, an approach for the selection of the optimal operating conditions for a generic mass transfer-limited liquid-liquid reaction was presented that could be applied to any solvent pair to achieve a desired conversion and flow rate.

2.6 Nomenclature

General		$[\boldsymbol{Units}]$
d_h	Hydraulic diameter	[mm]
D_A	Molecular diffusion coefficient of 4-NPA in the phase	[m^2/s]
H_A	Organic/aqueous concentration distribution coefficient of 4-NPA	
$K_{org}a$	Overall volumetric mass transfer coefficient	[s^{-1}]
l	Contraction length	[mm]
ΔP	Pressure loss across reactor	[Pa]
Q	Volumetric flow rate	[m^3/min]
w	Contraction width	[mm]
V	Volume	[mL]

Greek Symbols		
ε	Average rate of energy dissipation $(\Delta P/\rho\tau)$	$[m^2/s^3]$
α	Pre-exponential coefficient from fit model	
β	Exponential coefficient from fit model	
η	Conversion of reactant	
ϕ	volumetric phase fraction	
μ	Dynamic viscosity	$[Pa\ s]$
ρ	Fluid density	$[kg/m^3]$
τ	Average residence time	$[s]$
σ	Fluid interfacial tension with water	[N/m]

Indices	
R	Reactor
c	Continuous phase (aqueous in this case)
*	Evaluated at the onset of the drop flow regime

Acronyms	
RTC	Residence Time Channel

Acknowledgements

The authors would like to thank the Natural Sciences and Engineering Research Council of Canada, including the CREATE program in Continuous Flow Science, and Lonza AG for their financial contribution. Also, Ehrfeld Mikrotechnik BTS is acknowledged for the reactor manufacturing.

2.7 References

[1] P. Plouffe, A. Macchi, D.M. Roberge, From batch to continuous chemical synthesis-a toolbox approach, Org. Process Res. Dev. 18 (2014) 1286–1294. doi:10.1021/op5001918.

[2] P. Plouffe, D.M. Roberge, A. Macchi, Liquid–liquid flow regimes and mass transfer in various micro-reactors, Chem. Eng. J. 300 (2016) 9–19. doi:10.1016/j.cej.2016.04.072.

[3] E. Mielke, D.M. Roberge, A. Macchi, Microreactor mixing-unit design for fast liquid—liquid reactions, J. Flow Chem. 6 (2016) 279–287. doi:10.1556/1846.2016.00026.

[4] B. Ahmed, D. Barrow, T. Wirth, Enhancement of reaction rates by segmented fluid flow in capillary scale reactors, Adv. Synth. Catal. 348 (2006) 1043–1048. doi:10.1002/adsc.200505480.

[5] B. Ahmed-Omer, D. Barrow, T. Wirth, Effect of segmented fluid flow, sonication and phase transfer catalysis on biphasic reactions in capillary microreactors, Chem. Eng. J. 135 (2008) S280–S283. doi:10.1016/j.cej.2007.07.017.

[6] V.D. Parker, Instantaneous rate constants in physical organic chemistry: Application to acyl transfer reactions of p-nitrophenyl acetate to hydroxide ion, J. Phys. Org. Chem. 19 (2006) 714–724. doi:10.1002/poc.1064.

[7] P. Plouffe, D.M. Roberge, J. Sieber, M. Bittel, A. Macchi, Liquid–liquid mass transfer in a serpentine micro-reactor using various solvents, Chem. Eng. J. 285 (2016) 605–615. doi:10.1016/j.cej.2015.09.115.

[8] P. Plouffe, M. Bittel, J. Sieber, D.M. Roberge, A. Macchi, On the scale-up of micro-reactors for liquid–liquid reactions, Chem. Eng. Sci. 143 (2016) 216–225. doi:10.1016/j.ces.2015.12.009.

[9] S.S. Mongeon, D.M. Roberge, M. Bittel, P. Elsner, A. Macchi, Liquid–Liquid Mass Transfer in an Oscillatory-Flow Mesoscale Coil Reactor without Baffles, Org. Process Res. Dev. (2016) acs.oprd.5b00356. doi:10.1021/acs.oprd.5b00356.

[10] E. Mielke, P. Plouffe, N. Koushik, M. Eyholzer, M. Gottsponer, N. Kockmann, A. Macchi, D.M. Roberge, Investigation of Overall and Localized Heat Transfer in Curved Micro-Channel Reactor Systems, Submitt. to IJHMT. (2017).

3 Liquid-Liquid Mass Transfer in an Oscillatory-Flow Mesoscale Coil Reactor without Baffles

Sébastien S. Mongeon,[a] Dominique M. Roberge,[b] Michael Bittel,[b] Petteri Elsner,[b] and Arturo Macchi[a]

a, Centre for Catalysis Research and Innovation, Department of Chemical and Biological Engineering, University of Ottawa, K1N 6N5 Ottawa, Canada.

b, Chemical Manufacturing Technologies, Lonza AG, CH-3930 Visp, Switzerland.

This manuscript has been published Org. Process Res. Dev. 2016, 20, 733−741

ABSTRACT

Interphase mass transfer rates of an immiscible liquid−liquid system are investigated in an oscillatory-flow coil reactor without baffles. A baffle-less system is chosen since much research has been completed in baffled tubes with little performance comparison to baffle-less tubes, which offer lower operating and capital costs. In our experiments, interphase mass transfer rates are evaluated via the two-phase alkaline hydrolysis of 4-nitrophenyl acetate (4-NPA) in a toluene−water biphasic system. The mass transfer rate increased 7-fold at the maximum tested oscillation of 5,000 oscillatory-flow Reynolds number. The best application for the oscillatory-flow coil reactor is determined using a comparison to other liquid−liquid flow platforms in the presented toolbox approach. The oscillatory-flow coil reactor becomes a clear complement to a plate micro-reactor for gaining volume.

3.1 Introduction

A micro-reactor has become an essential tool in the development of flow processes in the fine chemical and pharmaceutical industry by enabling small flow rates and minimising reagents.[1] A plate micro-reactor is useful for reactions that are transport-limited requiring rapid mass and heat transfer rates. A plate with a proper structure is selected according to the phases of a reaction: homogeneous, liquid-liquid, or gas-liquid.[1] In such case, the cost per heat exchange area is attractive. However, upon scale-up, it is not the most appropriate reactor when a larger volume is required where the cost per volume may become prohibitive. In such case, a metallic tube/coil, from its simpler manufacturing technique, becomes the reactor of choice for flow technologies in which a volume gain is required. A tubular heat exchanger, a tube filled with static mixers/baffles, and a long packed column are all variations of tube/coil and its simplest generic form remains the most useful for: resistance to fouling, ease of cleaning and operation, and ultimately cost. This article will demonstrate that by a simple oscillation technique the coil reactor can become quite versatile enabling liquid-liquid reactions.

In continuous flow, mixing is categorised into passive and active mixing.[1,2] Passive mixing uses the energy input of the flow, i.e., pump or source of pressure, as the single source of mixing energy. The challenge in passive mixing comes from the compromise between selecting a production rate and obtaining the desired mixing as both properties are related to the same energy input. Active mixing uses an additional energy source to create mixing, e.g., pressure disturbance, electrokinetics, acoustic, and radiation, among

others.[2] The use of active mixing allows the independent manipulation of mixing intensity and residence time. This decoupling provides better control over the system to attain the desired mixing result at a chosen production rate.

Many types of mixing structures/arrangement in plate micro-reactors[2–5] and mesoscale or millimeter scale oscillatory baffled reactors (meso-OBR)[6,7] are currently being used to perform mixing of liquid-liquid systems. The suffix meso, meaning middle, is applied to represent the transition between the micro to macro area of reactors. These meso-OBR reactors generally have diameters smaller than 15 mm.[6]

Further research is needed in the area to determine the effect of flow oscillation on mass transfer in baffle-less tubes; to determine the transition point in flow regime[8,9] and its effect on mass transfer; and to obtain information for mesoscale reactors at oscillatory-flow Reynolds number in the turbulent-flow regime, typically in the range between 1000 and 10 000, since current studies in meso-OBR have not gone above 316.[6] This information will allow determining the best applications for the reactor when comparing other flow platforms such as plate micro-reactors and meso-OBR in a reactor selection toolbox approach.[1]

3.2 Flow Characterisation

Pulsatile and oscillatory-flow are respectively defined as when the net-flow is greater than the amplitude of the oscillating component (i.e., the flow is always positive) and when the net-flow is lesser than the amplitude of the oscillating component (i.e., a negative or reverse-flow component is present at a certain point in the cycle). Presented

in Figure 3.1, the relationship between the net-flow and superimposed pulsatile/oscillatory-flow is broken down into five cases.[9,10] The focus of this research is on the reverse pulsatile/asymmetrical oscillatory-flow.

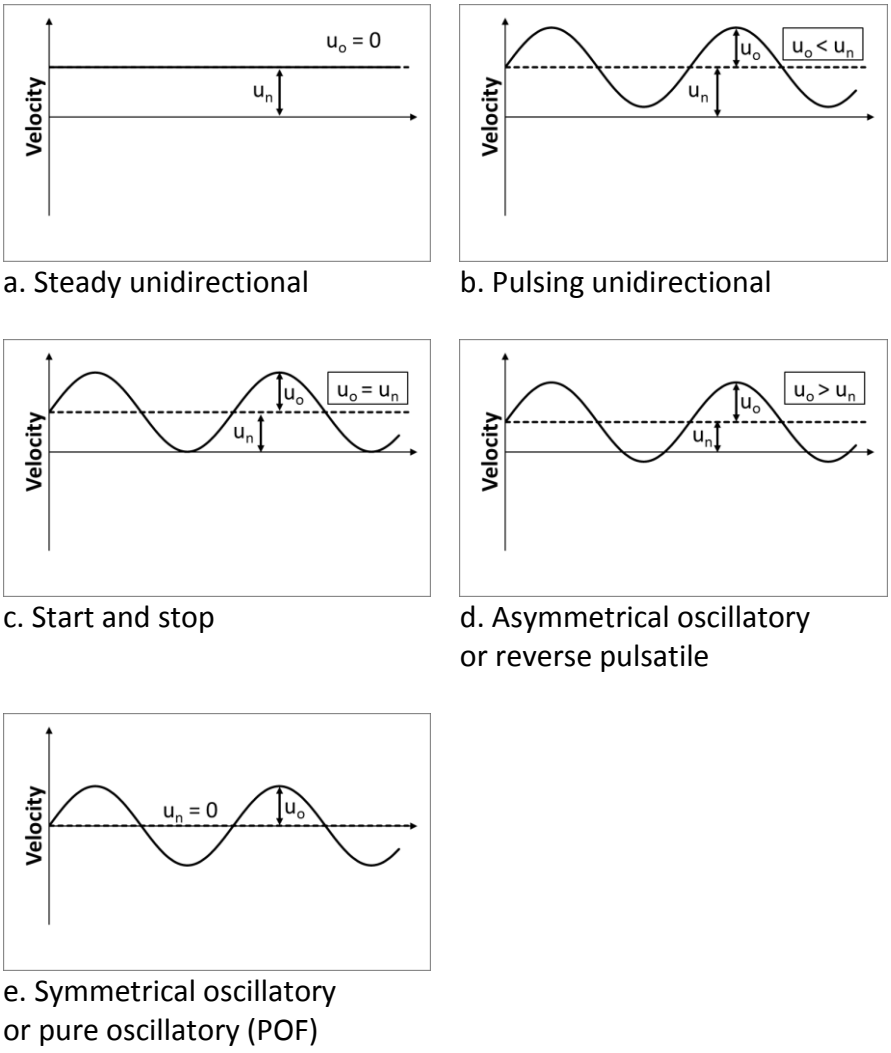

a. Steady unidirectional

b. Pulsing unidirectional

c. Start and stop

d. Asymmetrical oscillatory or reverse pulsatile

e. Symmetrical oscillatory or pure oscillatory (POF)

Figure 3.1. Types of pulsatile-flow**[9,10]**

The steady unidirectional flow has a constant net positive velocity with zero amplitude pulse, i.e., flow without pulsation. The pulsing unidirectional flow has a net velocity larger than the pulsation amplitude, which means that the fluid always move in the forward direction, cycling through acceleration and deceleration. The start and stop

flow is the transition between pulsatile and oscillatory-flow; it has a net-flow equal to the pulsation amplitude. The name “start and stop” describes the fluid coming to a stop at each cycle before starting its forward movement. The asymmetrical oscillatory flow has a net flow between zero and the oscillation amplitude; the fluid velocity is negative for a certain period of the oscillation, hence the reverse pulsatile-flow name. The symmetrical oscillatory-flow has no net-flow; the only flow component present is the oscillation. Symmetrical oscillatory-flow is the only type not considered to be in the continuous-flow category, it is an oscillatory batch process.

From dimensional analysis, an oscillatory-flow can be fully described with the three following dimensionless parameters:[11]

net-flow Reynolds number	$Re_n = \frac{\rho u_n d_{tube}}{\mu}$	(3.1)
oscillatory-flow Reynolds number	$Re_o = \frac{\rho u_o d_{tube}}{\mu}$	(3.2)
Womersley number	$Wo = \frac{d_{tube}}{2}\sqrt{\frac{\omega\rho}{\mu}}$	(3.3)

Using the dimensionless numbers Re_n, Re_o, and Wo, instead of standard units numbers u_n, u_o, and f allows comparison of the results between systems of different dimensions. The net-flow Reynolds number, Re_n shown in equation (3.1), enables comparison of scale and fluid component systems through the ratio of the inertial to the viscous forces. When used in conjunction with a pulsatile or an oscillatory component, it is referred to as either the mean,[12–14] average/time-average,[8,15] or net/net-flow[16–19]

Reynolds number. The term net-flow Reynolds number is chosen in this article due to its wider usage in literature.

The Reynolds number has also been applied to the pulsatile-flow component in multiple pulsatile and oscillatory systems. It is referred to as the pulsating Reynolds number[20] or the oscillating/oscillatory-flow Reynolds number, Re_o.[11,16,21–23] The term oscillatory-flow Reynolds number is chosen for its current wide usage in the literature; however, both consist of the same definition shown in equation (3.2). The velocity term is adapted from the net-flow Reynolds number. The net velocity, u_n, is replaced by the oscillatory velocity, u_o. The oscillation amplitude (centre-to-peak), x_o, which represents the length in the coil that a fluid packet travels during the oscillation, is transferred into a velocity using the angular frequency, ω. To obtain a single value from the constantly varying oscillating velocity, the oscillatory maximum velocity, $u_{o|max}$, is used. The maximum velocity is attained at every cycle when the sinusoidal component is equal to 1. Equations (3.4), (3.5), and (3.6) show the calculations describing the oscillatory velocity.

$$u_o = x_o \omega \sin(\omega t) \tag{3.4}$$

$$u_{o|max} = x_o \omega \tag{3.5}$$

$$\omega = 2\pi f \tag{3.6}$$

The third parameter to describe an oscillatory-flow is the Womersley number, Wo, shown in equation (3.3). Introduced in 1955, it evaluates the ratio of the transient inertial force of the oscillation to the viscous forces.[24] When the Womersley number

is larger than 10, the dominating forces are the oscillatory inertial forces.[25] Lower values indicate that the viscous forces are dominant and that the pressure and flow are synchronised.[24,26]

In all of the three previously described dimensionless parameters, the properties of the continuous phase, i.e., water, in which generated eddies can breakup the dispersed phase, are used to represent the liquid-liquid system. For the sake of conciseness and ease of reading, the mention of “continuous phase” with each term and in subscript will be omitted in the text.

3.3 Experimental Techniques

The selected reaction to perform the mass transfer tests is the alkaline hydrolysis of 4-nitrophenyl acetate (4-NPA), shown in Figure 3.2. It is currently used as a chemical method for interphase mass transfer rate evaluation.[4,27,28] The reported apparent pseudo first-order intrinsic rate constant for a concentration of 0.02 mol/L NaOH is 0.280 s^{-1} ,[29] which is already orders of magnitude greater than the expected overall volumetric interphase mass transfer coefficient and thus accomplishes the requirement that reaction kinetics are not rate-limiting for conversion. The stoichiometric ratio of the reaction is 2:1 ratio; however, to ensure a pseudo-first order reaction, a 9:1 ratio with the 4-NPA (0.05 mol/L) is chosen.

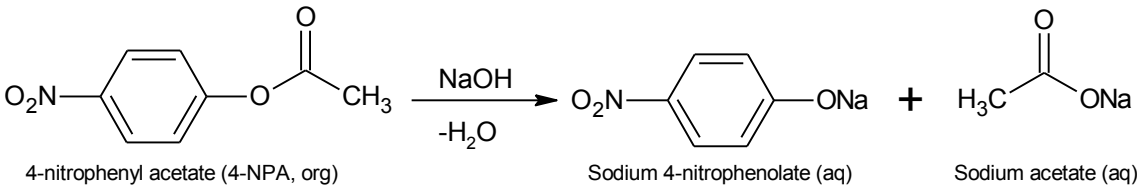

Figure 3.2. Alkaline hydrolysis of 4-nitrophenyl acetate.**[4]**

Toluene is used as the organic phase in the system for its relatively high interfacial tension with water, creating a very low-miscible biphasic system. Earlier studies have shown that this system can require residence/reaction times of several minutes making it a suitable reaction for reactors of larger volume such as a coil.[4] The properties of the toluene and 0.5 M of sodium hydroxide in water at 25 °C are shown in Table 3.1.

Table 3.1. Properties of Toluene and Water Used in the Biphasic Liquid-Liquid System

solvent	ρ **(kg/m^3)**	μ **(mPa·s)**	σ **with water (mN/m)**
toluene [30]	862	0.552	35.4
0.5 M NaOH in H_2O [31]	1020	1.124	-

The overview of the experimental setup is presented in Figure 3.3. The equi-massic feed flow is monitored by two Endress Hauser Promass 80A coriolis mass-flow meters. These are relayed in a feedback control loop to two Fuji HYM-08 metering pumps. The pulsatile-flow is generated by the LEWA LDB1 metering pump. The pulsator has a head diameter of 14 mm with an independently adjustable length and frequency. The maximum length and frequency of the piston are 15 mm and 3.6 Hz, respectively. In order to translate the piston amplitude to the pulsation length in the coil, the piston amplitude is multiplied by 9.4 (the ratio of the piston area over the transverse internal

coil area). A blind flange is installed on the inlet of the pump, while the outlet is connected with a T junction to the reactant feed line going to the reactor. No average positive flow is thus created by the pulsator pump; the same fluid is pushed back and forth into the pulsator.

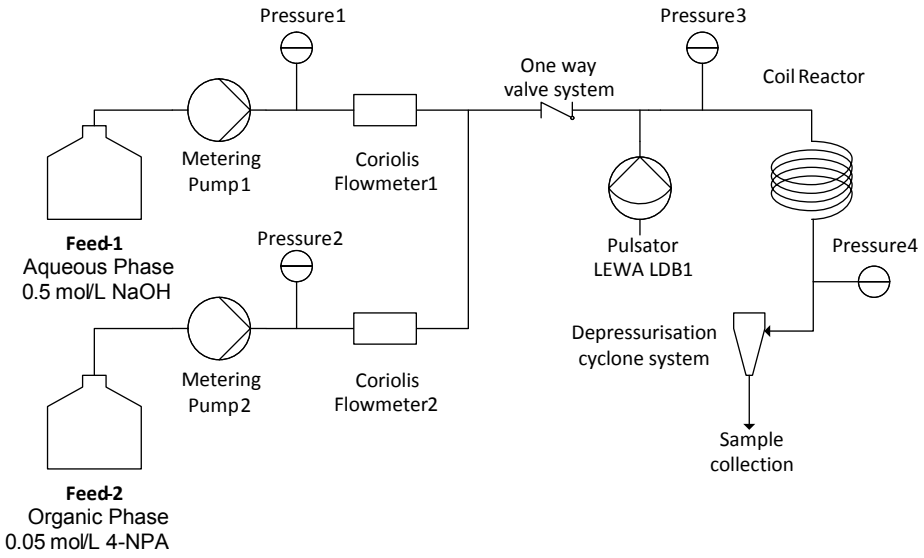

Figure 3.3. Experimental setup.

The 800 mL coil reactor is composed of a 48 m long tube with an inner diameter (ID) of 4.57 mm (1/4'' OD tube coil). The tube is coiled with a 295 mm diameter (centre-to-centre of tube) and a spacing of 10 mm between each turn of the coil. This spacing is present for an increased heat transfer capacity (not evaluated in this article). A coil schematic is presented in Figure 3.4 and a summary of the key parameters of the pulsator and coil is shown in Table 3.2.

Table 3.2. Dimensions of the Oscillatory-Flow Coil Reactor and Pulsator

details	units	values
d_{tube}	mm	4.57
V_{coil}	mL	800
d_{coil}	mm	295
d_{piston}	mm	14.0
$f_{piston\|max}$	Hz	3.6
$x_{piston\|max}$	mm	7.5
A_{piston}/A_{tube}	-	9.4
$x_{coil\|max}$	mm	70.4
Z_{coil}	m	48

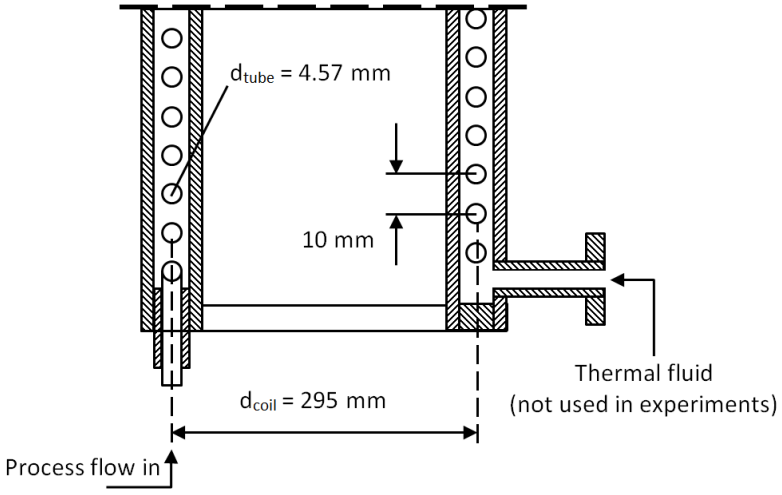

Figure 3.4. Cross-section schematic of the coil reactor.

Following the coil reactor, the back pressure is regulated with a restriction device and nitrogen (N_2) gas addition before the depressurisation cyclone. The backpressure is applied in order to avoid cavitation with the oscillatory-flow. The fluid is then depressurised to atmospheric pressure with the use of the cyclone system. The built-in-house cyclone has a diameter of 0.15 m and height of 0.30 m. The reaction samples are collected and allowed to settle for a short duration of 15 s for phase separation. An equal volume of 0.5 mL of aqueous and organic phase is pipetted into a quench solution

of 72.8 w/w% acetonitrile, 26.5 w/w% water, and 0.7 w/w% acetic acid. The acetic acid reacts with the NaOH in the aqueous phase to halt the possibility of the hydrolysis 4-nitrophenyl acetate reaction. The molar ratio of acetic acid to NaOH was set to 6:1. The conversion was determined using an HPLC calibration curve made using the response surface method. The HPLC system is composed of the HP Agilent 1100 series HPLC with a 250 mm 4.6 mm Agilent Zorbax SB-C8 column to separate the compounds.

Time to reach steady state is evaluated for the coil to determine the appropriate sampling time after a step change in operating set point. The first tests shown in Figure 3.5 are performed using multiple flow rates without oscillation. The second test shown in Figure 3.6 is performed using a piston frequency of 3.3 Hz and amplitude of 2.8 mm at a net-flow rate of 100 g/min. The solvents without reactants are filled into the coil in order to prime the system. The feeds are then changed to include the reactants while the chosen operating parameters are set. This is considered to be the starting time, i.e., t=0. The normalised residence times are calculated using the sample collection time at the outlet of the system divided by the system residence time at the operating conditions, which is estimated by taking the coil tube reactor volume divided by the net volumetric flow rate. The conversion result at each sampling time is normalised with (divided by) the average of the last three sample points of their respective test run.

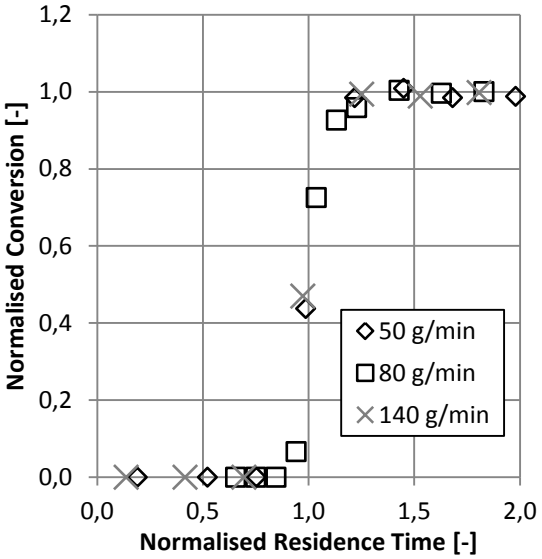

Figure 3.5. Time to steady state for the hydrolysis reaction without oscillation for multiple net-flow rates.

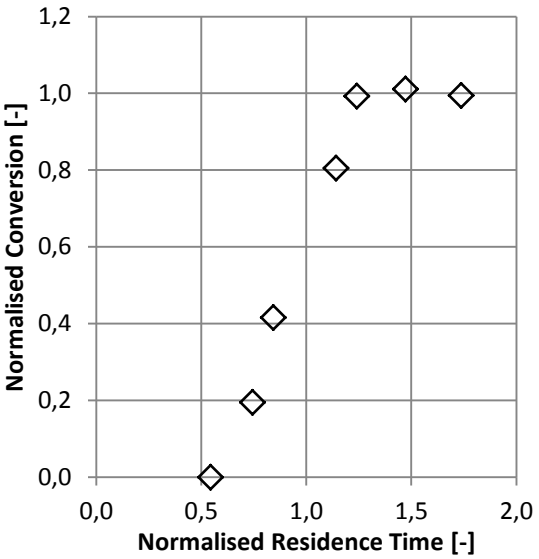

Figure 3.6. Time to steady state for the hydrolysis reaction with oscillation (net-flow rate of 100 g/min, piston amplitude of 2.8 mm, and frequency of 3.3 Hz).

The added oscillation created backmixing as shown by the earlier rise after ~0.5 normalised residence time in Figure 3.6; however, steady state is reached after ~1.3 normalised residence time in all of the cases. The samples during the following experiments were thus taken at time after 1.5 normalised residence time in order to minimise reactant use and ensure a reliable conversion result. At each operating condition, three distinct samples are collected at steady state with a minimum interval of 1 min between each one.

The chosen operating conditions evaluated are presented in Table 3.3 with the upper limit of the oscillatory-flow portion. The maximum oscillatory-flow Reynolds number is chosen to be an order of magnitude greater than that of the net-flow Reynolds number creating the desired oscillatory dominated reverse pulsatile flow system. The

Womersley number of the continuous phase is set to reach as close to 10 in order to have the oscillatory inertial forces dominate the viscous forces.[25] The frequency of the piston is operated at a maximum of 90% capacity (3.3 Hz) and the amplitude at 93% capacity (7.0 mm). In order to avoid cavitation during pressure oscillations caused by the oscillatory-flow, the system is kept under backpressure at the outlet of the coil reactor using N_2 gas and a line restriction device.

Table 3.3. Selected Operating Flow Conditions

operating parameter	units	net-flow	oscillatory-flow (maximum tested)
$\boldsymbol{Q}$	mL/min	63.3; 84.8; 105.5	1,180
$\boldsymbol{u}$	m/s	0.065; 0.086; 0.109	1.20
$\boldsymbol{Re}$	-	270; 357; 450	4,960
$\boldsymbol{Wo}$	-	-	9.9
$\boldsymbol{f}$	Hz	-	3.3
$\boldsymbol{x_{piston}}$	mm	-	7.0
$\boldsymbol{x_{coil}}$	mm	-	65.7

3.4 Results and Discussion

3.4.1 Conversion of the 4-Nitrophenyl Acetate Hydrolysis

The conversion for the alkaline hydrolysis of 4-NPA, η, is obtained at a net-flow rate of 80 g/min and a fixed frequency of 2.9 Hz. As shown in Figure 3.7, a 60 percentage point increase in conversion is obtained through a piston amplitude increase from 0.0 mm to 7.0 mm. The equivalent amplitude (centre-to-peak) in the coil is 0.0 mm to 65.7 mm.

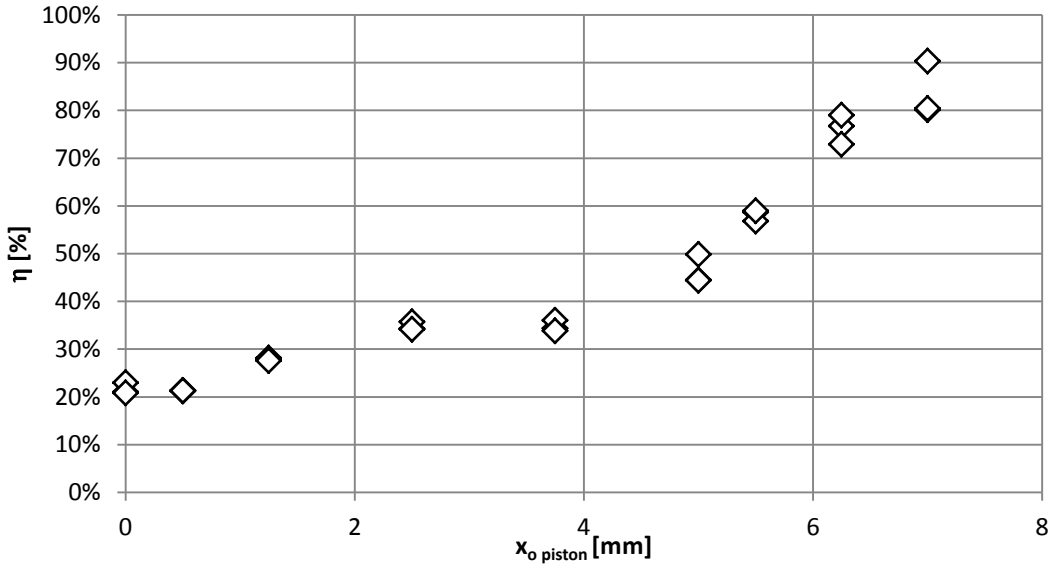

Figure 3.7. Hydrolysis conversion with varying piston amplitude (net-flow rate of 80 g/min and frequency of 2.9 Hz).

Typically, an increase of 8.5 percentage point in conversion is observed with the addition of the depressurisation cyclone system. The gain in conversion will affect positively the reported interphase mass transfer rate for the coil; however, the depressurisation component is an integral part of the system as the coil needs to operate under backpressure to avoid cavitation during pulsation. As such, the reported values of interphase mass transfer are of the overall reactor system rather than strictly the coil component.

3.4.2 Interphase Mass Transfer Rate in a Toluene-Water System

The overall volumetric mass transfer coefficient of the organic phase, $K_{org}a$, shown in equation (3.7) is calculated using a reactive extraction mass balance.[32] It is used to compare various reactor systems due to its normalised volume.[4] The assumption of the plug flow model is made. The equi-massic feed in the experiments gives a constant

volumetric organic phase fraction, φ_{org} , of 0.537, with the assumption that there is no slip velocity between the phases. The oscillation amplitude and frequency are put into dimensionless form using the oscillatory-flow Reynolds number.

$$K_{org}a = -\frac{\varphi_{org}}{\tau}\ln(1-\eta) \tag{3.7}$$

The overall volumetric mass transfer coefficient as a function of Reynolds number is shown in Figure 3.8. The frequency is kept constant at 2.9 Hz, while the pulsator amplitude is varied from 0.0 mm to 7.0. A 7-fold (6.7 times) increase in mass transfer rate is obtained from the no oscillation case (2.30 x 10^{-4} s^{-1}) to the oscillatory-flow Reynolds number of 4,976 at a piston displacement of 7.0 mm (1.53 x 10^{-3} s^{-1}).

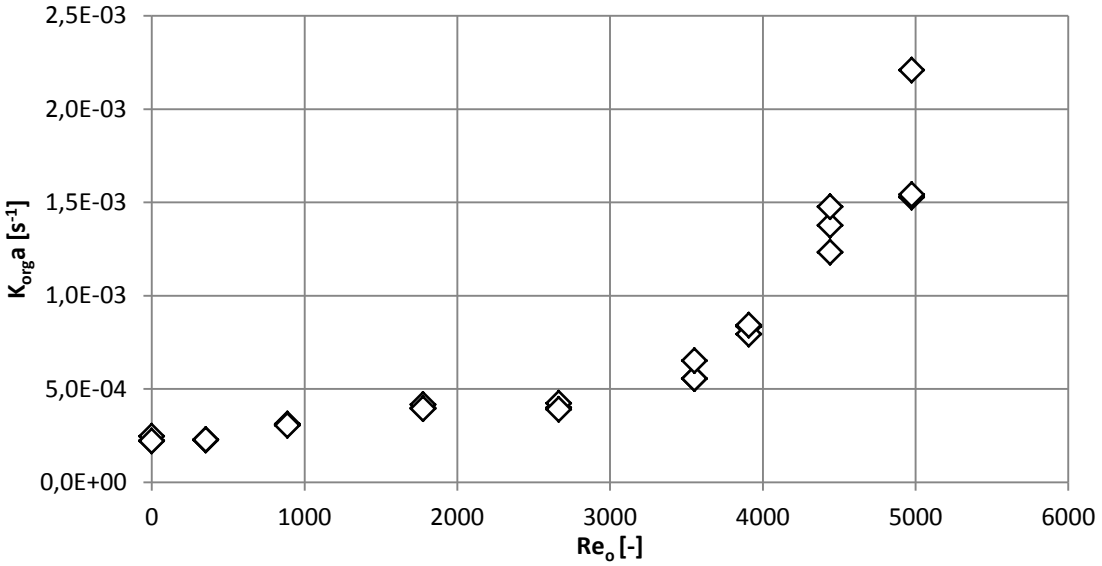

Figure 3.8. Overall volumetric mass transfer coefficient as a function of the oscillatory-flow Reynolds number (net-flow rate of 80 g/min and frequency of 2.9 Hz).

The overall volumetric mass transfer coefficient stays unchanged from an oscillatory-flow Reynolds number of 0 to 355. In this region, the flow type is a pulsing unidirectional

or very close to a start and stop-flow. When flow reversal occurs at an oscillatory-flow Reynolds number of 355, the interphase mass transfer rate begins to increase. This is in agreement with the mass transfer rate being dominated by the net-flow until flow reversal occurs.[33] It is also noticed that a distinct increase in the slope of the mass transfer coefficient occurs at a Reynolds number of ~2,670. From our experience and literature,[4] this slope increase indicates a change in flow regime. We propose that the flow is transitioning to a drop flow regime.

In the drop flow regime, the Sauter mean diameter can be estimated using equation (3.8), described and used with the same biphasic system and reaction by Plouffe et al.[34] The equation is derived from a stagnant spheres model with a fully developed concentration profile model and can be used since the reaction can be modeled as a fast pseudo-first order reactive extraction.[32] The estimation is used to validate that a droplet diameter smaller than that of the coil is obtained after transitioning to drop flow. The values used for the parameters are given in Table 3.4.

$$d_{32} = \frac{H_A D_{Ad}}{\sqrt{D_{Ac} k_{rxn} C_{Bc}}} \left(\sqrt{1 + \frac{12\varphi_d}{K_c a} \frac{D_{Ac} k_{rxn} C_{Bc}}{H_A D_{Ad}}} - 1 \right) \qquad (3.8)$$

At the transition to drop flow, a droplet size diameter of 1.7 mm is estimated. This diameter represents roughly a third of the 4.57 mm coil diameter. At the maximum oscillatory-flow Reynolds number, a droplet size diameter of 0.6 mm is obtained. From experience in micro-reactor plates, these values are far enough from the coil diameter

to avoid interaction with the wall to obtain for example slug flow. The relatively small droplet diameter corroborates the flow transitioning to a drop flow regime.

Table 3.4. Parameter Values for the Sauter Mean Diameter Calculation

parameter	description	value
D_{Ac}	molecular diffusion coefficient of 4-NPA in the continuous phase	6.32×10^{-10} m^2 s^{-1}
C_{Bc}	concentration of NaOH in the continuous phase	0.5 mol L^{-1}
H	organic/aqueous concentration distribution coefficient	229.81
k_{rxn}	second order reaction rate constant	14 m^3 mol^{-1} s^{-1}

3.4.3 Amplitude versus Frequency

In order to determine if the amplitude and frequency term are equal in mixing contribution, the evaluation of the mass transfer rate at a constant product of amplitude and frequency is completed, i.e., a constant oscillatory-flow Reynolds number. Three frequencies are arbitrarily chosen to span the operating range of the pulsator; 1.5, 2.2, and 3.3 Hz. Three constant products of pulsator amplitude and frequency are chosen; 5.4, 9.1, .and 10.9 mm·s^{-1} which have an oscillatory-flow Reynolds number equivalent to 1,330, 2,240 and 2,670, respectively. The plunger amplitude is then calculated to obtain the desired velocity product at each frequency.

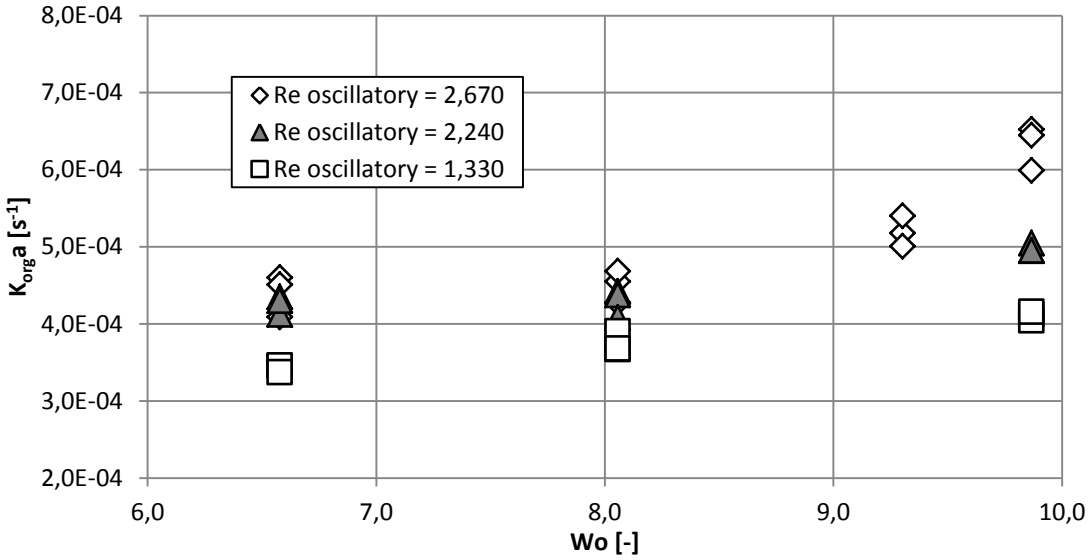

Figure 3.9. Overall volumetric mass transfer coefficient as a function of the Womersley number for three iso-oscillatory-flow Reynolds number curves.

As shown in Figure 3.9, the overall mass transfer coefficient increases with higher frequency (Wo number) for the three constant velocity (Re_o) curves. Thus, the frequency component shows a greater influence on the mass transfer rate than the amplitude. Similar results for an air-water system in an OBR are also reported in literature.[35]

It is noted that a higher pressure oscillation is experienced when using a higher frequency vs larger amplitude at equal oscillatory-flow Reynolds number. The transient inertial forces over the viscous forces are increasing with the increment in frequency and the higher pressure oscillation can be attributed to inertia and relaminarisation effects.[36] An increase in frequency at a constant amplitude results in a greater mass transfer rate compared to a proportional increase in amplitude at a constant frequency.

It is also noticed at the higher Womersley number of 10 (frequency of 3.3 Hz) the increase in overall mass transfer coefficient at a constant frequency is greater for an equivalent increase in oscillatory-flow Reynolds number than at the lower frequencies. This frequency is at the lower limit of the oscillatory inertia dominant regime at the Womersley number of 10, previously mentioned in the flow characterisation section.[25]

3.4.4 Reactor Performance Comparison

A clear choice for comparison is the OBR. It has all of the flow components of the oscillatory-flow coil with the addition of baffle type orifice inserts throughout the length of the tube. Steady research has been completed on the OBR since the end of the 1980s[20,22] and meso-OBR have also been studied since 2003.[6] However, reported experiments in meso-OBR have used low continuous phase oscillatory-flow Reynolds number of 36 to 316 in liquid-liquid systems of vegetable oil and methanol in the transesterification to produce biodiesel,[37–39] and no mass transfer rates are reported. As such, no clear comparison can be made with an OBR of similar dimensions for an immiscible liquid-liquid system. Reported single phase liquid and biphasic gas-liquid are presented below, followed by toluene-water mass transfer rates in micro-reactor plates.

Mackley and Ni reported a 10-fold increase in dispersion number for a water system in a 25 mm tube in the range of 100 to 1,800 oscillatory-flow Reynolds number.[40] Hewgill et al. reported a 6-fold increase in mass transfer rates for an air-water system using an

oscillatory-flow Reynolds number of 0 to 7,840 in a 26 mm tube diameter. No increase was noticed using an oscillation in a tube without baffles.[41] Ni and Gao reported a 5–6-fold increase in mass transfer rates for an air-water system in a 50 mm and 100 mm diameter OBR. In the 50 mm diameter OBR, the minimum oscillation was 3 Hz and 4 mm and the maximum oscillation was 8 Hz at 12 mm. In the 100 mm diameter OBR, the minimum oscillation was 2 Hz and 5 mm, and the maximum oscillation was 6 Hz at 12 mm.[35]

To compare the obtained interphase mass transfer rate of the oscillatory-flow coil on an absolute value basis, reported results of a toluene-water system in two micro-reactor plates, the Sickle and the SZ FlowPlate by Ehrfeld Mikrotechnik BTS, are used.[4] The sickle is an obstacle-based micro-mixer while the SZ is a curvature-based micro-mixer; these are shown in Figure 3.10 and Figure 3.11. The dimensions at the contraction in width by depth of the Sickle and SZ are, respectively, 0.20 x 0.50 mm and 0.50 x 1.25 mm. The contraction is indicated by the arrow in the figures. The reported results are shown alongside the obtained oscillatory-flow coil results in Figure 3.12. The secondary horizontal axis of the flow rate for the micro-reactor plates does not have a direct relationship with the primary horizontal axis of the Reynolds number used for the coil. Both axes are chosen to represent the operating range of each system. The comparison of the reactor systems is also completed using the average energy dissipation rate.

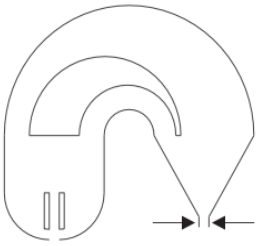

Figure 3.10. Sickle micro-mixer structure.

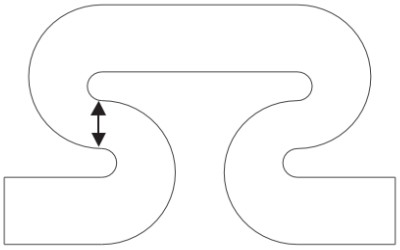

Figure 3.11. SZ micro-mixer structure.

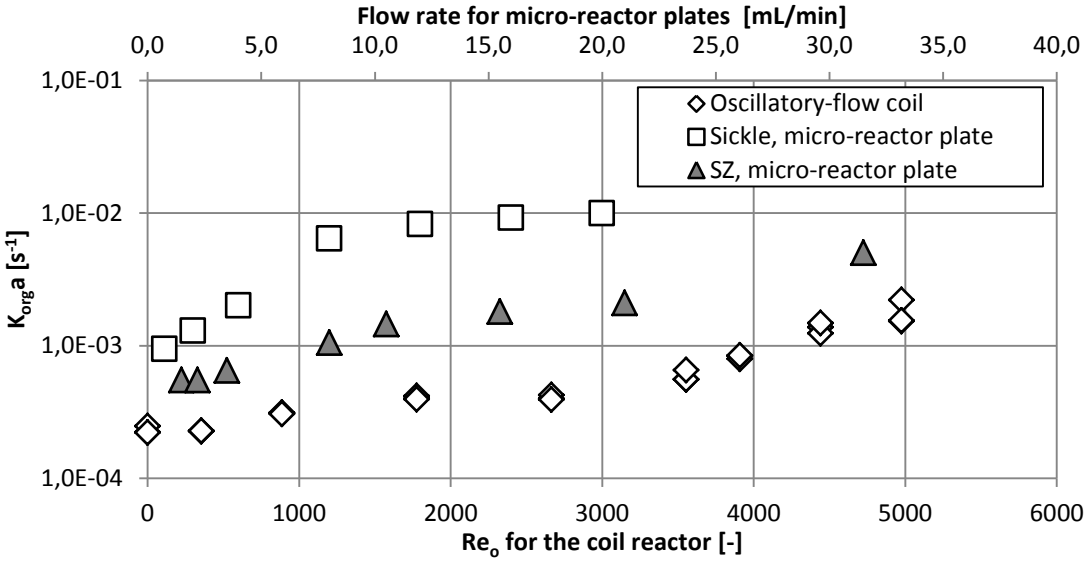

Figure 3.12. Oscillatory-flow coil overall mass transfer coefficient comparison with other micro-reactors (micro-reactor plate results from Plouffe et al. 2015).**[4]**

The average energy dissipation rate for the system, shown in equations (3.9) and (3.10) and graphically in Figure 3.13, is estimated using the sum of the net-flow[4] and the oscillatory energy dissipation rate component.[42] The referenced oscillatory energy dissipation rate is divided by the density due to the original units being reported in W m^{-3} instead of the W kg^{-1}, and the phase angle (δ) is considered to be zero (we assumed pressure and velocity to be in-phase). The average energy dissipation rate for

the referenced micro-reactor plates is calculated using the net-flow average energy dissipation rate shown in the first term of equation (3.10).

$$\bar{\varepsilon} = \bar{\varepsilon}_n + \bar{\varepsilon}_o \tag{3.9}$$

$$\bar{\varepsilon} = \frac{\Delta P_n}{\rho \cdot \tau} + \frac{1}{2}\frac{\Delta P_o \cos(\delta)\, x_o \omega}{Z \cdot \rho} \tag{3.10}$$

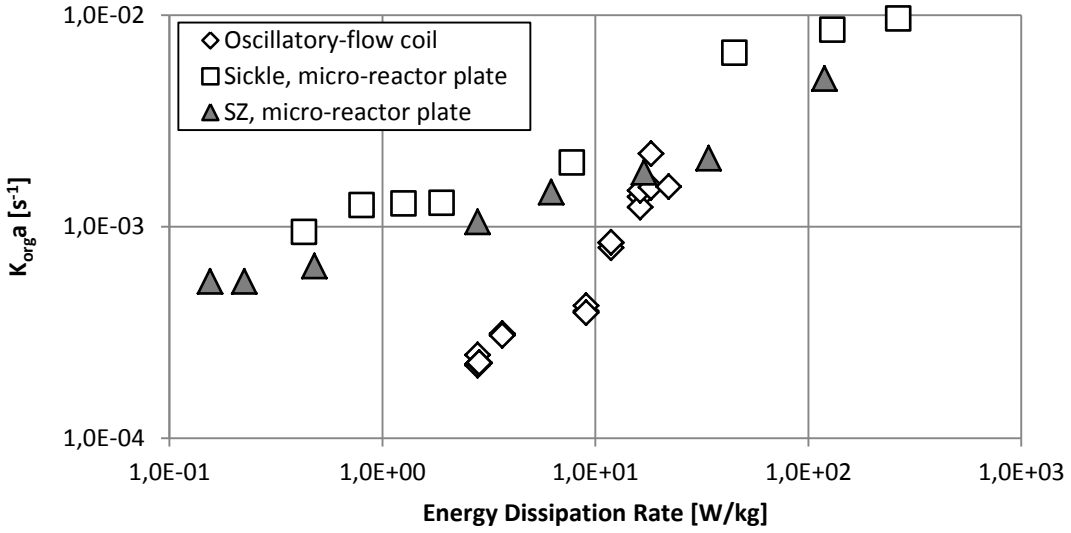

Figure 3.13. Oscillatory-flow coil overall mass transfer coefficient micro-reactor comparison as a function of the average energy dissipation rate (micro-reactor plate results from Plouffe et al. 2015)**[4]**

The mass transfer performance of a plate micro-reactor and an oscillatory-flow coil reactor become similar when the flow enters the drop flow regime. Moreover, for the oscillatory-flow reactor, this is likely the transition between laminar and turbulent flow as depicted in Figure 3.8. Prior to drop flow regime, the oscillatory-flow coil reactor underperforms relative to the plate micro-reactor. This is most likely due to its intrinsic milli-structure where the beneficial effect from the micro-structure (large phase

interfacial area due to geometry) is reduced. The mass transfer performance of a plate micro-reactor and an oscillatory-flow coil reactor becomes similar once the flow regime enters drop flow. Within its typical operating range (see Figure 3.12), a micro-reactor will provide greater $K_{org}a$ at corresponding energy dissipation rates making it a more suitable reactor for very fast reactions (Type A, see section 4.5 for reaction types). This is also applicable to heat transfer as micro-reactors have a greater intrinsic area ($m^2\ m^{-3}$). On the other hand, the oscillatory-flow reactor provides significantly greater volume at a reduced energy dissipation rate and $K_{org}a$ but can still operate in the same flow regime (drop flow) as the plate micro-reactor. In such case, the oscillatory-flow coil reactor becomes a clear complement to a plate micro-reactor for gaining volume, which naturally leads to an association with slower reactions. It can thus be used jointly (often Type B reactions) or independently (often Type C reactions) to the plate micro-reactor (Table 3.5).

3.4.5 Integration to the Micro-Reactor Toolbox

The micro-reactor toolbox[1] previously proposed by this group and shown in Table 3.5 uses reaction rates and phase types to determine the appropriate reactor to select. The three reactions rates, presented as type A, B, and C, are ordered respectively from the very fast type A (seconds) to the slow type C (several minutes).[43–45]

Table 3.5. Micro-Reactor Toolbox: Flow Modules for Reaction Types**[1]**

rates/phases	homogeneous	liquid-liquid	gas-liquid	solid-liquid
Type A	- plate SZ	- plate LL - plate HEART	- plate Venturi with TG mixing units	- CSTR - packed bed
Type B	- plate SZ - coil	- plate LL - plate HEART - pulsated coil	- plate Venturi with TG mixing units - static mixer - coil pressure	- CSTR - packed bed
Type C	- static mixer - coil	- static mixer - pulsated coil	- coil pressure	- pulsated coil

The previously proposed usage of the pulsated/oscillatory-flow coil for type B and C in liquid-liquid system holds true; however, as previously demonstrated through mass transfer rate performance, there is a clear overlap between the performance of a plate and coil that enables a smooth transition between both technologies or even a hybrid use (first a plate for when the reaction requires elevated transport rates, then a coil for the volume and residence time gain). Not shown in the toolbox is the ease of adaptability in volumes and relative low cost of production for the coil compared to micro-reactor plates.

There are still research areas in need of further investigation such as

- the impact of net-flow rate on overall volumetric mass transfer coefficient
- the effect of scale on mass transfer rate; the influence of higher oscillatory-flow Reynolds number using smaller diameter tubes

- the system operability with solid presence and/or fixed bed catalyst incorporation
- the overall volumetric mass transfer coefficient for different organic phase
- the heat transfer capacity.

3.5 Conclusions

The use of a baffle-less oscillatory-flow mesoreactor proved to be successful in increasing the mass transfer rate of a low miscibility biphasic liquid-liquid system of toluene and water. A 7-fold increase in interphase mass transfer rate is obtained compared to the unidirectional-flow base case, i.e., without oscillation. A proportional increase in oscillation frequency compared to amplitude results in a higher mass transfer rate. Mass transfer rates reach the lower end of the plate micro-reactor performance. Thus, a baffle-less oscillatory-flow mesoreactor can be used in low miscibility liquid-liquid systems as a complement to the plate type micro-reactor and typically to gain volume for longer reaction times.

3.6 Nomenclature

General Symbols

a	Specific interfacial area	[m^{-1}]
A	Cross-sectional area	[m^2]
C_{ij}	Concentration of molecule ‘‘i” in phase ‘‘j”	[mol m^{-3}]
d	Diameter	[m]
d_{32}	Sauter mean diameter	[m]
D_{ij}	Molecular diffusion coefficient of molecule ‘‘i” in the phase ‘‘j”	[m^2 s^{-1}]
f	Frequency of oscillation	[Hz]
H	Organic/aqueous concentration distribution coefficient	[-]
ID	Inner diameter	[m]
k_{rxn}	second order reaction rate constant	[m^3 mol^{-1} s^{-1}]
K	Overall mass transfer coefficient	[m s^{-1}]
$K_c a$	Overall volumetric mass transfer coefficient of the continuous phase	[s^{-1}]
$K_{org} a$	Overall volumetric mass transfer coefficient of the organic phase	[s^{-1}]
OD	Outer diameter	[m]
P	Pressure	[Pa]
Q	Volumetric flow rate	[m^3 s^{-1}]
Re	Reynolds number	[-]
t	Time	[s]
u	Superficial velocity	[m s^{-1}]
V	Volume	[m^3]
Wo	Womersley number	[-]
Z	Coil length	[m]

Greek Symbols

δ	Phase angle between pressure and velocity (time between peaks multiplied by the angular frequency)	[rad]
$\bar{\varepsilon}$	Average energy dissipation rate	[W kg^{-1}]
η	Conversion of 4-NPA	[%]
μ	Dynamic viscosity	[Pa s]
ρ	Density	[kg m^{-3}]
σ	Interfacial tension	[N m^{-1}]
τ	Residence time	[s]
φ	Volumetric phase fraction	[-]
x	Centre-to-peak amplitude	[m]
ω	Angular frequency	[rad s^{-1}]

Indices

A	4-nitrophenyl acetate
aq.	Aqueous phase
B	Sodium hydroxide base
c	Continuous phase
coil	Coil properties of the oscillatory-flow coil reactor
d	Dispersed phase
max.	Maximum
n	Net-flow component
o	Oscillatory-flow component
org.	Organic phase
piston	Piston of the pulsator
tot.	Total of continuous and dispersed phase
tube	Tube properties of the oscillatory-flow coil reactor

Acknowledgement

A special mention is made to Lonza AG for its financial contribution and laboratory use and the laboratory technician Anton Pfammatter, the CREATE program in Continuous Flow Science (NSERC), for the financial support to promote continuous-flow research

3.7 References

[1] Plouffe, P., Macchi, A., and Roberge, D. M., 2014, "From Batch to Continuous Chemical Synthesis - A Toolbox Approach," Org. Process Res. Dev., **18**, pp. 1286–1294.

[2] Nguyen, N.-T., and Wu, Z., 2005, "Micromixers — A Review," J. Micromech. Microeng., **15**, pp. R1–R16.

[3] Plouffe, P., Macchi, A., and Donaldson, A. A., 2013, "Enhancement of Interphase Transport in Mini-/Microscale Applications Using Passive Mixing," Heat Transf. Eng., **34**, pp. 159–168.

[4] Plouffe, P., 2015, "Micro-Reactor Design for Fast Liquid- Liquid Reactions," University of Ottawa.

[5] Kashid, M. N., Renken, A., and Kiwi-Minsker, L., 2011, "Gas-Liquid and Liquid-Liquid Mass Transfer in Microstructured Reactors," Chem. Eng. Sci., **66**, pp. 3876–3897.

[6] McDonough, J. R., Phan, A. N., and Harvey, A. P., 2015, "Rapid Process Development Using Oscillatory Baffled Mesoreactors – A State-of-the-Art Review," Chem. Eng. J., **265**, pp. 110–121.

[7] Reis, N, Harvey. A.P, M. M. ., 2005, "Fluid Mechanics and Design Aspects of a Novel Oscillatory Flow Screenong Mesoreactor.pdf," Trans IChemE, **83(A4)**, pp. 357–371.

[8] Özdinç Çarpinlioğlu, M., and Yaşar Gündoğdu, M., 2001, "A Critical Review on Pulsatile Pipe Flow Studies Directing towards Future Research Topics," Flow Meas. Instrum., **12**, pp. 163–174.

[9] Nabavi, M., and Siddiqui, K., 2010, "A Critical Review on Advanced Velocity Measurement Techniques in Pulsating Flows," Meas. Sci. Technol., **21**, p. 042002 (19pp).

[10] Southard, J., 2006, "Oscillatory Flow," *An Introduction to Fluid Motions, Sediment Transport, and Current-Generated Sedimentary Structures*, Boston, pp. 184–200.

[11] Peacock, J., Jones, T., Tock, C., and Lutz, R., 1998, "The Onset of Turbulence in Physiological Pulsatile Flow in a Straight Tube," Exp. Fluids, **24**, pp. 1–9.

[12] Trip, R., Kuik, D. J., Westerweel, J., and Poelma, C., 2012, "An Experimental Study of Transitional Pulsatile Pipe Flow," Phys. Fluids, **24**.

[13] Gebreegziabher, T., Sparrow, E. M., Abraham, J. P., Ayorinde, E., and Singh, T., 2011, "High-Frequency Pulsatile Pipe Flows Encompassing All Flow Regimes," Numer. Heat Transf. Part A, **60**, pp. 811–826.

[14] Einav, S., and Sokolov, M., 1993, "An Experimental Study of Pulsatile Pipe Flow in the Transition Range," J. Biomech. Eng., **115**, pp. 404–411.

[15] Trabelsi, F., 1993, "Pulsatile Flow in a Conical Tube," University of Ottawa.

[16] Ni, X., 1995, "A Study of Fluid Dispersion in Oscillatory Flow through a Baffled Tube," J. Chem. Technol. Biotechnol., **64**, pp. 165–174.

[17] Smith, K. B., and Mackley, M. R., 2006, "An Experimental Investigation into the Scale-up of Oscillatory Flow Mixing in Baffled Tubes," Chem. Eng. Res. Des., **84**, pp. 1001–1011.

[18] Palma, M., and Giudici, R., 2003, "Analysis of Axial Dispersion in an Oscillatory-Flow Continuous Reactor," Chem. Eng. J., **94**, pp. 189–198.

[19] Lobry, E., Lasuye, T., Gourdon, C., and Xuereb, C., 2015, "Liquid–liquid Dispersion in a Continuous Oscillatory Baffled Reactor – Application to Suspension Polymerization," Chem. Eng. J., **259**, pp. 505–518.

[20] Ni, X., and Gough, P., 1997, "On the Discussion of the Dimensionless Groups Governing Oscillatory Flow in a Baffled Tube," Chem. Eng. Sci., **52**, pp. 3209–3212.

[21] Ni, X., and Mackley, M. R., 1993, "Chemical Reaction in Batch Pulsatile Flow and Stirred Tank Reactors," Chem. Eng. J. Biochem. Eng. J., **52**, pp. 107–114.

[22] Ni, X., Mackley, M. R., Harvey, A. P., Stonestreet, P., Baird, M. H. I., and Rama Rao, N. V., 2003, "Mixing Through Oscillations and Pulsations - A Guide to Achieving Process Enhancements in the Chemical and Process Industries," Trans IChemE, **81**, pp. 373–383.

[23] Xia, Q., 2012, "Enhancement of Liquids Mixing Using Active Pulsation in the Laminar Flow Regime," University of Manchester.

[24] Womersley, J. R., 1955, "Method for the Calculation of Velocity, Rate of Flow and Viscous Drag in Arteries When the Pressure Gradient Is Known," J. Physiol., **127**, pp. 553–563.

[25] Fazle Hussein, A. K. M., and Settler, J. C., 1986, "On Transition of the Pulsatile Pipe Flow," J. Fluid Mech., **170**, pp. 169–197.

[26] McDonald, D. A., 1974, *Blood Flow in Arteries*, London.

[27] Ahmed, B., Barrow, D., and Wirth, T., 2006, "Enhancement of Reaction Rates by Segmented Fluid Flow in Capillary Scale Reactors," Adv. Synth. Catal., **348**, pp. 1043–1048.

[28] Ahmed-Omer, B., Barrow, D., and Wirth, T., 2008, "Effect of Segmented Fluid Flow, Sonication and Phase Transfer Catalysis on Biphasic Reactions in Capillary Microreactors," Chem. Eng. J., **135**, pp. 280–283.

[29] Parker, V. D., 2006, "Instantaneous Rate Constants in Physical Organic Chemistry: Application to Acyl Transfer Reactions of P-Nitrophenyl Acetate to Hydroxide Ion," J. Phys. Org. Chem., **19**, pp. 714–724.

[30] Backes, H. M., Jing Jun, M., E., B., and G., M., 1990, "Interfacial Tensions in Binary and Ternary Liquid—liquid Systems," Chem. Eng. Sci., **45**, pp. 275–286.

[31] Alexandrov, A. A., 2005, "The Equations for Thermophysical Properties of Aqueous Solutions of Sodium Hydroxide," *14th International Conference on the Properties of Water and Steam*, Kyoto, pp. 86–90.

[32] Levenspiel, O., 1999, *Chemical Reaction Engineering*, Wiley, New York.

[33] Howell, J. A., and Finnigan, S. M., 1991, "Hydrodynamics and Membrane Filtration," *Effective Industrial Membrane Processes: Benefits and Opportunities*, E. Turner, ed., Springer Netherlands, pp. 49–60.

[34] Plouffe, P., Roberge, D. M., Sieber, J., Bittel, M., and Macchi, A., 2016, "Liquid–liquid Mass Transfer in a Serpentine Micro-Reactor Using Various Solvents," Chem. Eng. J., **285**, pp. 605–615.

[35] Ni, X., and Gao, S., 1996, "Scale-up Correlation for Mass Transfer Coefficients in Pulsed Baffled Reactors," Chem. Eng. J. Biochem. Eng. J., **63**, pp. 157–166.

[36] Ribas, F. A., and Deschamps, C. J., 2004, "Friction Factor Under Transient Flow Condition," *International Compressor Engineering Conference*, Purdue University, West Lafayette, pp. 1–8.

[37] Phan, A. N., Harvey, A. P., and Eze, V., 2012, "Rapid Production of Biodiesel in Mesoscale Oscillatory Baffled Reactors," Chem. Eng. Technol., **35**, pp. 1214–1220.

[38] Zheng, M., Skelton, R. L., and Mackley, M. R., 2007, "Biodiesel Reaction Screening Using Oscillatory Flow Meso Reactors," Process Saf. Environ. Prot., **85**, pp. 365–371.

[39] Phan, A. N., Harvey, A. P., and Rawcliffe, M., 2011, "Continuous Screening of Base-Catalysed Biodiesel Production Using New Designs of Mesoscale Oscillatory Baffled Reactors," Fuel Process. Technol., **92**, pp. 1560–1567.

[40] Mackley, M. R., and Ni, X., 1991, "Mixing and Dispersion in a Baffled Tube for Steady Laminar and Pulsatile Flow," Chem. Eng. Sci., **46**, pp. 3139–3151.

[41] Hewgill, M. R., Mackley, M. R., Pandit, A. B., and Pannu, S. S., 1993, "Enhancement of Gas-Liquid Mass Transfer Using Oscillatory Flow in a Baffled Tube," Chem. Eng. Sci., **48**, pp. 799–809.

[42] Mackley, M. R., and Stonestreet, P., 1995, "Heat Transfer and Associated Energy Dissipation for Oscillatory Flow in Baffled Tubes," Chem. Eng. Sci., **50**, pp. 2211–2224.

[43] Roberge, D. M., Gottsponer, M., Eyholzer, M., and Kockmann, N., 2009, "Industrial Design, Scale-Up, and Use of Microreactors," Chem. Today, **27**, pp. 8–11.

[44] Roberge, D. M., Ducry, L., Bieler, N., Cretton, P., and Zimmermann, B., 2005, "Microreactor Technology: A Revolution for the Fine Chemical and Pharmaceutical Industries?," Chem. Eng. Technol., **28**, pp. 318–323.

[45] Kockmann, N., Gottsponer, M., and Roberge, D. M., 2011, "Scale-up Concept of Single-Channel Microreactors from Process Development to Industrial Production," Chem. Eng. J., **167**, pp. 718–726.

4 Conclusions and Future Work

4.1 Conclusions

Passive and active mixing mechanisms have been studied in this thesis with respectively two types of micro-reactors: a micro-reactor plate with four configurations of a static mixing element having a contraction size of 500 µm by 1,250 µm; and a pulsed coil reactor with a diameter of 4,570 µm. The mixing efficiencies of the two systems were objectively compared using the interphase mass transfer rates determined through the reaction of the two-phase alkaline hydrolysis of 4-NPA. The work provides demonstration of the appropriate application for each reactor system in a fast liquid-liquid reaction.

The tested micro-reactors proved suitable to generate an unstable emulsion in an immiscible liquid-liquid system. The desired operating conditions were proposed for each reactor design in the passive mixing geometrical rearrangement of the mixing elements using an interspaced residence time channel. The active mixing using pulsed secondary flow in a micro-reactor without obstacles reactor proved to be successful in increasing the mass transfer rate in an immiscible *toluene-water* biphasic system and can be used as a complement to the plate type micro-reactor.

In section 2 of the thesis, passive mixing mechanism is explored with geometrical optimisation of the static mixing elements arrangement. Four micro-reactor plates of A5 dimensions (148 mm x 210 mm) were manufactured using different spacing arrangements between the LL-Rhombus type static mixing elements. Four liquid-liquid

solvent pairs ranging in miscibility as well as in interfacial tension (1.8 to 35.4 mN/m) with water were used: *n-butanol-water*, *n-hexanol-water, MTBE-water*, and t*oluene-water*. The drop flow regime in each solvent pair was achieved at similar average energy dissipation rate for the different geometrical arrangement. Moreover, for a given solvent pair, the mass transfer coefficient was only a function of the energy dissipation rate once the drop flow regime was established. In practice, the drop flow regime first occured in the geometrical arrangement without the residence time channel which suggests droplet re-coalescence in the residence time channel; however, the different arrangements with the same number of mixing-units did not yield significantly different results. The ratio of mixing-unit to the residence time channel volume is a greater factor than the residence time channel. An approach for the selection of the optimal operating conditions for a generic mass transfer-limited liquid-liquid reaction was presented based on operating near the transition to drop flow as this is where conversion is maximum.

In section 3 of the thesis, an active mixing mechanism is explored with a secondary pulsed flow in a continuous flow coiled reactor. The *toluene-water* is used as the immiscible biphasic system as it presents the lower limiting system previously explored. A reactor system capable of reaching an oscillatory-flow Reynolds number of 5,000 was successfully fabricated. The maximum flowrate tested reached 105.5 mL/min while the maximum secondary pulsed flow was ten times higher at 1,180 mL/min. It was determined that the frequency parameter of the secondary pulsed flow is more important to increase mass transfer rate than a proportional amplitude increase. A 7-fold increase in interphase mass transfer rate was obtained when using the secondary

pulsed flow; the volumetric interphase mass transfer coefficients (10^{-3} s^{-1}) reach the lower end of the micro-reactor plate performance. Therefore, this reactor becomes complementary for chemical synthesis requiring longer residence times.

4.2 Future Work

The presented work in this thesis has highlighted novel micro-reactors for liquid-liquid reactions. Here are proposed subsequent research works in regards to the geometrical arrangement:

1. Further explore the recoalescence in the geometrical arrangement of the mixing units vs. residence time channel volume using:
    a. gas-liquid systems
    b. other mixing unit design
    c. different residence time channel geometries
2. Include the knowledge of the residence time channel in the succeeding geometric optimisation of the reactor designs.

Additional research avenues are proposed below in order to advance knowledge in secondary pulsed flow future works:

1. The system operability with solid presence or fixed bed catalyst incorporation
2. The heat transfer hot spot avoidance capacity of the system
3. The impact of net-flow rate on overall volumetric mass transfer coefficient
4. The effect of scale on mass transfer rate and the influence of higher oscillatory-flow Reynolds number using smaller diameter tube
5. The overall volumetric mass transfer coefficient for different organic phase

End of document